EEE Transactions on Aerospace and Electronic Systems, Available online 18 July 2023
DOI: 10.1109/TAES.2023.3296566


# Three-Dimensional Guidance Method with Course Modification for Altitude Shaping in Endoatmospheric Interception

Namhoon Cho

**Abstract**

This study presents a three-dimensional guidance law for the interception of an endoatmospheric target. The proposed method takes an empirical design approach which first specifies the structure of the lateral acceleration command as that of a linear optimal guidance law for zero-effort-miss nullifcation. Then, the direction of pursuit and the guidance gain are designed in accordance with the physical understandings of the motion characteristics of an aerodynamically-controlled interceptor. More specifically, the proposed method induces an intentional increase in the flight altitude around the initial phase while respecting the maximum altitude constraint, all of which are realised through modification of the desired flight path angle in the vertical plane. The proposed guidance method does not rely on explicit definition of design elements such as engagement planes, guidance phases, complicated time-to-go estimation, and waypoints. Moreover, the proposed design approach of modifying the desired course based on the collision courses naturally facilitates smooth handover to the terminal phase near the collision condition. Numerical simulation shows that the proposed guidance method is effective in intercepting a nonmanoeuvring target over a wide range of engagement conditions to the target in comparison to the existing guidance laws developed for homing and midcourse flight.

**Index Terms**

course modification, final speed, guidance, interception, three-dimensional

## I. Introduction

The intention behind the observed motion of a flying object like aircraft that can manoeuvre in both longitudinal and lateral directions cannot be perfectly known in a non-cooperative setting. For this reason, aerodynamically-controlled missiles for interception of endoatmospheric aircraft targets should be able to perform a large manoeuvre that exceeds the manoeuvre capability of the target in the terminal homing

Namhoon Cho is with the Centre for Autonomous and Cyber-Physical Systems, School of Aerospace, Transport and Manufacturing, Cranfield University, Cranfield, MK43 0AL, Bedfordshire, United Kingdom. e-mail: nhcho91@gmail.com

phase. This is necessary to cancel out the effect of imperfect target trajectory prediction in the midcourse phase and to form an advantageous engagement geometry. In these respects, increasing the final speed of an interceptor is generally accepted as desirable for increasing the kill probability even in the case of the target performing manoeuvres.

The flight time is relatively long for long-range anti-air missiles that should counteract targets approaching from far distances. Large errors are unavoidable in the predicted trajectories of the missile and the target for the time-to-go that are necessary to accurately compute the ideal collision course at each instance. This is because the prediction error accumulates over time in proportion to the length of the prediction horizon and the amount of speed change experienced by the missile throughout the boost and glide phases is quite significant. Therefore, it is not reasonable to apply various guidance laws developed mainly for the terminal homing situation by leveraging finite-horizon linear quadratic optimal error regulation formulations to the midcourse phase of a long-range flight. Many different engineering approximations can be introduced to reduce the trajectory prediction error and to obtain closed-form expressions for the integrals such as time-to-go that appear in the prediction equations. However, the design complexity of approximate solution methods is high while the expected performance is hardly good enough due to the accumulated effect of nonlinear models of thrust, aerodynamics, and atmosphere. In summary, accurate prediction of the impact point is very difficult if the duration of the flight is long. Trajectory prediction using numerical integration at each instance is not realistic. Also, convexification-based online trajectory optimisation still requires more research on its reliability.

Maintaining the altitude at a high level where the air density is low enough for reducing drag is desirable to increase the final speed of endoatmospheric interceptors. However, the maximum altitude should be limited under a specified ceiling since aerodynamic control becomes ineffective due to the thin air at altitudes higher than about 30km above the ground. One possible strategy for the design of the midcourse guidance algorithm is to place a waypoint at the point of maximum altitude below the ceiling and set the desired incidence direction to be parallel to the ground surface. However, this methodology requires a massive offline trajectory optimisation process to compute the waypoint as a table indexed by the position of the predicted impact point (PIP). Also, the offline trajectory optimisation needs to be repeated whenever the model data for missile dynamics is updated.

Various approaches have been developed to address the midcourse guidance problem, especially for anti-air missiles. Characteristics of the optimal trajectories depending on the choice of performance index and the distance to the target were examined in [1]. A heuristic design approach that entails the manoeuvre pattern to deliberately increase the altitude considering the aerodynamic effects was investigated in [2]–[8]. The issues arising from the trajectory prediction error implicit in the basic proportional navigation

guidance law (PNG) were addressed. Singular perturbation control approach was applied to the midcourse guidance problem in [9]–[11]. The analytical design of kappa guidance laws based on simplifying approximations and the linear optimal control theory was presented in [12], [13]. Optimal-control-based midcourse guidance laws were also studied in [14]–[17] without considering the physical dependencies of aerodynamics on flight altitude. More recently, methods for maximisation of final speed were developed in [18] based on online sequential convex programming and in [19] based on the combination of offline trajectory optimisation and waypoint guidance for online implementation.

Design of a midcourse guidance algorithm that is suitable for long-range anti-air missiles is challenging because of the necessity to address multiple requirements at the same time. First, the complexities in predicting impact points for a target located at a long distance from the launch position demand to avoid too heavy dependence on the highly uncertain PIP. Second, the difficulties in generating closed-loop trajectory that maintains high-altitude cruising in the middle without exceeding the maximum altitude limit, intercepts the target at the final time, and promotes higher final speed demand to have a separate control over altitude. Lastly, computationally efficient and simple algorithm is much preferred in practice.

To the best of author's knowledge, an algorithm taking all of the above requirements into account is hardly found in the open literature. The guidance laws based on zero-effort-miss formulation and optimal control such as those presented in [3], [4], [8], [12]–[15] provide analytical expression for the lateral acceleration command which is desirable for implementation and verification. However, most of the midcourse guidance methods introduced above rely on an externally supplied PIP for their operation. Regarding the shaping of altitude, Sec. VII-B in [3] discussed an idea for vertical-axis control to meet a given maximum altitude with the zero-effort trajectory. However, the idea cannot be applied identically as a means to limit the altitude to other methods that perform vertical manoeuvres to increase the flight path angle in the initial phase instead of tracking the zero-effort trajectory. Also, the section on "Modified Guidance Formulation" in [4] described a guidance law that introduces an additional flight path angle with respect to the so-called generalised collision course as a heuristic for increasing the final speed. However, the guidance law was developed without considering satisfaction of the maximum altitude limit.

With this background, this study aims to devise a guidance method which can deal with multiple aspects of the long-range midcourse guidance problem for moving target interception. More specifically, this study places emphasis on the following design considerations:

- Generation of a curved path in vertical plane with altitude shaping to increase final speed
- Generation of a near-straight path in horizontal plane to reduce flight time for greater final speed
- Satisfaction of a maximum altitude limit to avoid loss of aerodynamic control effectiveness
- Independence from explicit specification of manoeuvre plane, guidance phases, and waypoints

- Applicability to a wide range of flight distances
- Applicability to vertical launch condition
- Smooth switching of manoeuvre strategy to the PNG

The main contribution of this study is to present a simple three-dimensional guidance law that can be applied to a wide range of engagement conditions for long-range anti-air missiles. The proposed approach exploits the command structure similar to that of linear optimal guidance laws for zero-effort-miss nullification. The specific novelty of the proposed approach lies at the combination of heuristic modifications introduced into the design of the vertical course correction algorithm for altitude shaping and the feedback gain. The modification considers the trajectory characteristics of aerodynamically-controlled interceptors. The desired course direction is updated at each instance in the vertical plane by modifying the ideal collision course computed using a simplified kinematic model, e.g., constant velocity model. Also, the proposed method is structured so that the modified desired course direction gradually approaches the ideal collision course as the trajectory prediction horizon becomes short enough to validate the modelling approximation. It does not demand the interceptor to follow the ideal collision course from the beginning of long-distance midcourse guidance phase.

Overall, the proposed method is more reasonably understood as a practical approach that involves empirical/heuristic design choices rather than as a result of theoretically rigorous design. It is intended to achieve certain balance between many requirements. This study presents a numerical experiment for different initial positions and headings of the target to validate the proposed method. A three-dimensional point-mass dynamics model introducing the angular velocity of lift acceleration is used to provide sufficient fidelity to assess the performance of three-dimensional guidance laws. The test case of the simulation also includes comparison of the proposed method with the pure PNG and the course modification guidance law of [4].

## II. Guidance Method

This section presents a three-dimensional guidance law based on the pursuit of the desired flight direction vector. The desired flight direction vector for the midcourse phase is constructed by computation of the ideal collision course followed by modification of the desired vertical flight path angle to allow for the objective of increasing final speed as well as the maximum altitude limit. Lateral acceleration command is then generated in the direction to align the current missile velocity vector with the desired flight direction vector.

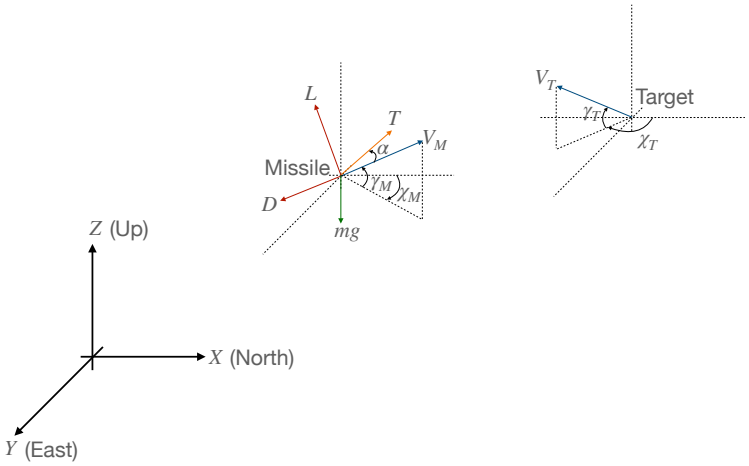


Fig. 1. Definition of Coordinate System and Variables for Three-Dimensional Point-Mass Model

### *A. Problem Formulation and Basic Concepts*

Consider the coordinate system and the variables defined as shown in Fig. 1. The ground-fixed coordinate system follows the East-North-Up convention, and the flat earth model is considered for simplicity of guidance law design and performance analysis. Subscripts $M$ and $T$ refer to the missile and the target, respectively. Also, $V$, $\gamma$, and $\chi$ denote speed, vertical flight path angle, and horizontal flight path angle, respectively.

The real aircraft target performs longitudinal/lateral manoeuvres as needed to avoid dangers or to fulfil its mission. However, it is impossible to perfectly identify the intention behind the manoeuvre of a non-cooperative target. For the aircraft propelled by an air-breathing engine, cruising speed variation is not large and the range of possible variation in the velocity direction appears to be approximately symmetric with respect to the velocity. In this sense, the trajectory predicted by assuming that the aircraft target does not perform lateral manoeuvre can be roughly viewed as an average of all possible predicted trajectories. Hence, this study assumes a constant velocity motion model for target trajectory prediction.

The kinematic equations for the motion of the missile and target can be described as

$$\begin{aligned} \dot{\mathbf{r}}_M &= \mathbf{v}_M \\ \dot{\mathbf{v}}_M &= \mathbf{a}_M = -c\left(t\right)\mathbf{v}_M + \mathbf{u}_M + \mathbf{g} \\ \dot{\mathbf{r}}_T &= \mathbf{v}_T \\ \dot{\mathbf{v}}_T &= \mathbf{0} \end{aligned} \tag{1}$$

In Eq. (1), $\mathbf{r}$, $\mathbf{v}$, and $\mathbf{a}$ represent position, velocity, and acceleration vectors, respectively, and the overdot

notation indicates the derivative with respect to time $t$. The term $-c(t)\,\mathbf{v}_M$ represents the component of acceleration vector due to thrust and drag which is parallel with $\mathbf{v}_M$, $\mathbf{u}_M$ denotes the lateral acceleration command that should be achieved by generating lift which is perpendicular to $\mathbf{v}_M$, and $\mathbf{g}$ is the constant gravitational acceleration.

Integrating the second row of Eq. (1) from the current instance $t$ to some final moment $\tau$ yields

$$\mathbf{v}_M(\tau) = \phi(\tau,t)\,\mathbf{v}_M(t) + \int_t^\tau \phi(\tau,\xi)\,(\mathbf{u}_M(\xi)+\mathbf{g})\,d\xi \tag{2}$$

where

$$\phi(\tau,t) = \exp\left[-\int_t^\tau c(\eta)\,d\eta\right] \tag{3}$$

Substitution of Eq. (2) into the first row of Eq. (1) followed by integration from the current instance $t$ to some final moment $t_f$ gives

$$\begin{aligned}\mathbf{r}_M(t_f) &= \mathbf{r}_M(t) + \int_t^{t_f} \mathbf{v}_M(\tau)\,d\tau \\ &= \mathbf{r}_M(t) + \int_t^{t_f}\left[\phi(\tau,t)\,\mathbf{v}_M(t) + \int_t^\tau \phi(\tau,\xi)\,(\mathbf{u}_M(\xi)+\mathbf{g})\,d\xi\right]d\tau \\ &= \mathbf{r}_M(t) + \int_t^{t_f}\phi(\tau,t)\,d\tau\mathbf{v}_M(t) + \int_t^{t_f}\int_t^\tau \phi(\tau,\xi)\,d\xi d\tau\mathbf{g} + \int_t^{t_f}\int_t^\tau \phi(\tau,\xi)\,\mathbf{u}_M(\xi)\,d\xi d\tau\end{aligned} \tag{4}$$

Integrating the third row of Eq. (1) from the current instance $t$ to some final moment $t_f$ considering nonmanoeuvring target model with constant $\mathbf{v}_T$ yields

$$\mathbf{r}_T(t_f) = \mathbf{r}_T(t) + \mathbf{v}_T t_{go} \tag{5}$$

where $t_{go} := t_f - t$. By defining the relative position of the target with respect to the missile which is often called the line-of-sight vector as $\mathbf{r} = \mathbf{r}_T - \mathbf{r}_M$, the relative position at $t_f$ corresponds to the interception error and it can be written as

$$\mathbf{r}(t_f) = \mathbf{r}(t) + \mathbf{v}_T t_{go} - \int_t^{t_f}\phi(\tau,t)\,d\tau\mathbf{v}_M(t) - \int_t^{t_f}\int_t^\tau \phi(\tau,\xi)\,d\xi d\tau\mathbf{g} - \int_t^{t_f}\int_t^\tau \phi(\tau,\xi)\,\mathbf{u}_M(\xi)\,d\xi d\tau \tag{6}$$

The interception error that will be attained when the missile does not perform any manoeuvre for course correction during the time interval $[t,t_f]$ corresponds to the zero-effort-miss (ZEM). The ZEM vector $\mathbf{z}(t)$ defined with respect to the prediction at the instance $t$ is the $\mathbf{r}(t_f)$ obtained by substituting $\mathbf{u}_M = \mathbf{0}$ in Eq. (6), which can be expressed as

$$\mathbf{z}(t) = \mathbf{r}(t) + \mathbf{v}_T t_{go} - \int_t^{t_f}\phi(\tau,t)\,d\tau\mathbf{v}_M(t) - \int_t^{t_f}\int_t^\tau \phi(\tau,\xi)\,d\xi d\tau\mathbf{g} \tag{7}$$

The ideal collision course is defined as the direction of missile velocity calculated at each instance $t$ along which the missile can intercept the target at $t_f$ without accelerating in the lateral direction to

perform path correction manoeuvres. Provided that all other variables remain fixed, the ideal collision course vector at $t$ can be obtained by finding the missile velocity that nullifies the ZEM vector as

$$\mathbf{v}_{ICC}(t) = \frac{\mathbf{r}(t) + \mathbf{v}_T t_{go} - \int_t^{t_f} \int_t^{\tau} \phi(\tau, \xi)\, d\xi d\tau \mathbf{g}}{\int_t^{t_f} \phi(\tau, t)\, d\tau} \tag{8}$$

### *B. Design of Guidance Law Based on Approximations*

From this point onward, the design approach will introduce rough approximations and simplifications considering the physical response characteristics rather than adhering to the theoretical rigour to prioritise the achievement of the guidance objectives.

*1) Consideration of Speed Variation:* Although $\mathbf{g}$ in Eq. (1) has a component in the direction parallel to $\mathbf{v}_M$, neglecting its presence leads to an approximate relation given by $c(t) \approx -\frac{\dot{V}_M}{V_M}$. Note that the same approximation was employed in [4]. With this approximation, the following relation also holds.

$$\phi(\tau, t) \approx \exp\left[-\int_t^{\tau} -\frac{dV_M(\eta)/d\eta}{V_M(\eta)} d\eta\right] = \exp\left[\int_t^{\tau} \frac{dV_M(\eta)}{V_M(\eta)}\right] = \frac{V_M(\tau)}{V_M(t)} \tag{9}$$

Let us define the time average of the missile speed for the interval $[t, t_f]$ as

$$\bar{V}_M(t) = \frac{1}{t_{go}} \int_t^{t_f} V_M(\tau)\, d\tau \tag{10}$$

The definite integral of $\phi(\cdot, \cdot)$ which is necessary to evaluate Eq. (8) can be obtained by leveraging the integration of Eq. (9) along with Eq. (9) as

$$\int_t^{t_f} \phi(\tau, t)\, d\tau \approx \frac{1}{V_M(t)} \int_t^{t_f} V_M(\tau)\, d\tau = \frac{\bar{V}_M(t)}{V_M(t)} t_{go} \tag{11}$$

By substituting Eq. (11) into Eq. (8) and neglecting the effect of gravitational acceleration, the collision course corresponding to the straight-line flight model for the predicted missile motion can be obtained as

$$\mathbf{v}_{SCC}(t) = \frac{\mathbf{r}(t) + \mathbf{v}_T t_{go}}{\frac{\bar{V}_M(t)}{V_M(t)} t_{go}} \tag{12}$$

Solving the equality condition given by $\|\mathbf{v}_{SCC}(t)\| = V_M(t)$ for $t_{go}$ leads to the following relation.

$$t_{go_{SCC}} = \frac{\mathbf{v}_T \cdot \mathbf{r}(t) + \sqrt{(\mathbf{v}_T \cdot \mathbf{r}(t))^2 + \left(\bar{V}_M^2(t) - V_T^2\right) \|\mathbf{r}(t)\|^2}}{\bar{V}_M^2(t) - V_T^2} \tag{13}$$

The speed change due to thrust and drag can be estimated with explicit numerical integration using the dynamic model information. However, repeating online prediction of the trajectory until the final time at each guidance command update cycle demands a substantial amount of computation. Also, the integration error accumulates over time in any case when the length of the prediction horizon is long because of the long distance to the true target that can perform manoeuvres. As a consequence, in the

case of an unpredictably manoeuvring aircraft target, the performance in terms of interception error will not always be improved even if the speed of the missile can be predicted accurately. In this regard, online computation of the average future speed $\bar{V}_M(t)$ at each instance is impractical.

Meanwhile, it is desirable for the long-range anti-air missiles to fly along a near-straight course on the horizontal plane before the seeker can capture the target. This requirement is motivated from the viewpoint of energy management to reduce the amount of flight time and the horizontal manoeuvre. It is well-known that the straight line collision course obtained by assuming constant velocity motion for both the target and the missile, i.e., the model which verifies $\bar{V}_M(t) = V_M(t)$, corresponds to the ideal collision course of the PNG. If the PNG that considers the true target as the aiming point is applied as the horizontal guidance algorithm from the beginning of the midcourse phase, the horizontal path flown by the missile will be a curve if the speed of the missile varies over time even if the true velocity of the target is constant. By considering a pre-computed PIP as a virtual stationary target in the horizontal guidance algorithm before switching over to the homing phase, the path from the launch point to the PIP may appear to be close to a straight line on the horizontal plane. However, this design approach relies on the computation of the PIP for a wide range of engagement conditions. Also, the missile cannot accurately achieve a favourable engagement geometry for homing guidance at the end of the midcourse phase if the pre-computed PIP involves large discrepancies from the actual target motion.

In summary, physically consistent determination of $\bar{V}_M$ that enters into Eq. (13) by viewing it as one of the design parameters instead of the accurate value for the average future speed will suffice the purpose of generating a near-straight horizontal course toward a nonmanoeuvring target during the majority of the midcourse phase. To this end, one possible approach is to set $\bar{V}_M(t)$ to be a nominal speed $V_{\text{nominal}}$, e.g., a value similar to (maximum fire range) / (maximum flight time), until the missile approaches sufficiently close to the target, and then switch its value to $V_M(t)$ within a specified distance from the target to perform more accurate homing by similarly moving in space as it has been guided by the PNG. One specific example is as follows:

$$\bar{V}_M(t) = f_{sw}^{lin}\left(\frac{\|\mathbf{r}(t)\|}{\|\mathbf{r}(t_0)\|}; \rho_{sw_0}, \rho_{sw_f}\right) V_{\text{nominal}} + \left(1 - f_{sw}^{lin}\left(\frac{\|\mathbf{r}(t)\|}{\|\mathbf{r}(t_0)\|}; \rho_{sw_0}, \rho_{sw_f}\right)\right) V_M(t) \tag{14}$$

where $f_{sw}^{lin}$ is a linear switching function which is defined as

$$f_{sw}^{lin}(x; x_{\max}, x_{\min}) = \max\left(\min\left(\frac{x - x_{\min}}{x_{\max} - x_{\min}}, 1\right), 0\right) \tag{15}$$

Note that the switching action of $f_{sw}^{lin}$ in Eq. (14) begins as soon as $\|\mathbf{r}(t)\|$ becomes smaller than $\rho_{sw_0}\|\mathbf{r}(t_0)\|$ and ends when $\|\mathbf{r}(t)\|$ reaches $\rho_{sw_f}\|\mathbf{r}(t_0)\|$.

*2) Modification of Collision Course Vector:* Provided that the lateral acceleration command is generated in the direction to align the missile velocity vector with the direction of the collision course computed at each update cycle, climbing and descending manoeuvres in the vertical plane can be achieved by modifying the vertical flight path angle of the collision course. The pattern of the vertical plane motion that increases altitude in the initial phase to fly through thin air and then starts descending as the missile approaches the target is desirable for increasing the final speed of the missile. By approximately incorporating the effect of gravitational acceleration that was neglected in the derivation of straight collision course in Eq. (12) and using $t_{go_{SCC}}$ given by Eq. (13), the gravity-assisted collision course can be obtained as follows:

$$\mathbf{v}_{GCC}(t) = \frac{\mathbf{r}(t) + \mathbf{v}_T t_{go_{SCC}} - \frac{1}{2}\mathbf{g} t_{go_{SCC}}^2}{\frac{\bar{V}_M(t)}{V_M(t)} t_{go_{SCC}}} \tag{16}$$

Equation (16) shows that the gravity-assisted collision course always has a larger component in the $Z$-axis of the ground-fixed coordinate system as compared to the straight collision course, thus pointing at a higher direction. Therefore, reduction of the lift acceleration with the aid of gravitational acceleration utilised for turning as well as altitude increase effect can be achieved by aligning the velocity with $\mathbf{v}_{GCC}$. However, reduction of the interception error should be more prioritised as the missile approaches close to the target, even at the cost of sacrificing the lift acceleration reduction or the altitude increase effects. The curved zero-effort trajectory following the direction specified by $\mathbf{v}_{GCC}$ is to perform projectile motion subject to gravity and drag for interception. For this reason, pursuit of $\mathbf{v}_{GCC}$ prefers the motion with absolute acceleration of $1g$ in the downwards direction. Prioritising certain direction of lateral acceleration is not desirable to deal with uncertainties in the end of engagement.

Hence, it is reasonable to switch the collision course from $\mathbf{v}_{GCC}$ to $\mathbf{v}_{SCC}$ in a similar manner to the switching structure designed for $\bar{V}_M(t)$ when the distance to the target becomes sufficiently small. One example design that applies the switching concept can be represented as

$$\mathbf{v}_{CC0}(t) = \begin{cases} \mathbf{v}_{SCC}(t) & \text{if } \|\mathbf{r}(t)\| < \rho_{sw_f} \|\mathbf{r}(t_0)\| \text{ and } |\gamma_{SCC}(t) - \gamma_{GCC}(t)| < \epsilon_{CC} \\ \mathbf{v}_{GCC}(t) & \text{otherwise} \end{cases} \tag{17}$$

where $\gamma_{SCC}$ and $\gamma_{GCC}$ are the vertical flight path angles for the collision course vector of Eqs. (12) and (16), respectively, and $\epsilon_{CC}$ is a small positive constant that defines a threshold for switching. Note that the vertical flight path angle can be expressed as

$$\gamma_{(\cdot)} = \operatorname{atan2}\left(\mathbf{v}_{(\cdot)} \cdot \hat{\mathbf{k}}, \sqrt{\left(\mathbf{v}_{(\cdot)} \cdot \hat{\mathbf{i}}\right)^2 + \left(\mathbf{v}_{(\cdot)} \cdot \hat{\mathbf{j}}\right)^2}\right), \qquad \text{for } (\cdot) \in \{SCC, GCC, CC0\} \tag{18}$$

The maximum altitude should be constrained below a certain threshold since the aerodynamic control surfaces lose effective control power for an altitude above 30km. To limit the maximum altitude, if the

vertical flight path angle $\gamma_{CC0}(t)$ that corresponds to the collision course $\mathbf{v}_{CC0}(t)$ has a positive value at a high altitude, the vertical flight path angle reference can be modified to reduce its value as the gap between the current altitude and certain altitude limit $Z_{\max}$ decreases so that it becomes zero at $Z_{\max}$. It is sufficient to prevent only excessive climbing without the necessity to restrict descending. A logic designed for modifying the desired vertical flight path angle from $\gamma_{CC0}$ to $\gamma_{MCC}$ is described in Algorithm 1. Note that $n$, $Z_{\text{act}}$, and $L$ in Algorithm 1 are the design parameters introduced to allow some degrees-of-freedom for trajectory shaping where $Z_{\text{act}} < Z_{\max}$, and $f_{sw}^{lin}$ is the linear switching function defined in Eq. (15). At each instance, the modification in Algorithm 1 applies a multiplicative correction to the original desired vertical flight path angle $\gamma_{CC0}$ if $\gamma_{CC0} \geq 0$ and $Z_M \leq Z_{\max}$. Here, the correction factor $f_{h_{\lim}}$ attains its value between 0 and 1 depending on the region where $Z_M$ lies due to the activation of switching function $f_{sw}^{lin}$. For $Z_M \leq Z_{\text{act}}$, we have $f_{h_{\lim}} = 1$, hence no correction is applied to $\gamma_{CC0}$. As $Z_M$ increases above the activation threshold $Z_{\text{act}}$, we have $f_{h_{\lim}} < 1$, which leads to the modified flight path angle satisfying $\gamma_{MCC} < \gamma_{CC0}$ for reducing the desired ascending rate. The correction factor satisfies $f_{h_{\lim}} = 0$ at $Z_M = Z_{\max}$. If $\gamma_{CC0} \geq 0$ and $Z_M > Z_{\max}$, Algorithm 1 prioritises altitude control to meet the maximum altitude constraint by specifying a negative value for $\gamma_{MCC}$.

**Algorithm 1:** Desired Vertical Flight Path Angle

**Output:** $\gamma_{MCC}(t)$

$f_{h_{\lim}} = \cos^2\left(\left\{f_{sw}^{lin}\left(Z_M(t); Z_{\max}, Z_{\text{act}}\right)\right\}^n \frac{\pi}{2}\right)$

**if** $\gamma_{CC0}(t) \geq 0$ **then**

  **if** $Z_M(t) \leq Z_{\max}$ **then**

    $\gamma_{MCC}(t) = f_{h_{\lim}} \gamma_{CC0}(t)$

  **else**

    $\gamma_{MCC}(t) = -\arcsin\left(\min\left(\frac{Z_M(t) - Z_{\max}}{L}, 1\right)\right)$

  **end**

**else**

  $\gamma_{MCC}(t) = \gamma_{CC0}(t)$

**end**

With no further modification applied to the desired horizontal flight path angle, the unit vector in the direction of the modified collision course that incorporates the modified desired vertical flight path angle can be obtained as

$$\hat{\mathbf{v}}_{MCC}(t) = \cos\gamma_{MCC}(t)\,\hat{\mathbf{i}}_{MCC}(t) + \sin\gamma_{MCC}(t)\,\hat{\mathbf{k}} \tag{19}$$

where

$$\hat{\mathbf{i}}_{MCC}(t) = \frac{\left(\hat{\mathbf{k}} \times \mathbf{v}_{CC0}(t)\right) \times \hat{\mathbf{k}}}{\left\| \left(\hat{\mathbf{k}} \times \mathbf{v}_{CC0}(t)\right) \times \hat{\mathbf{k}} \right\|} \tag{20}$$

with $\mathbf{v}_{CC0}(t)$ given by Eq. (17) and $\hat{\mathbf{k}} = \begin{bmatrix} 0 & 0 & 1 \end{bmatrix}^T$ representing the unit vector in the upward direction, i.e., $Z$-axis of the ground-fixed coordinate system.

*3) Construction of Command and Feedback Gain:* Finally, the lateral acceleration command can be constructed to have the same structure as the pursuit guidance law which steers the missile velocity $\mathbf{v}_M$ to the modified collision course $\hat{\mathbf{v}}_{MCC}$ as

$$\mathbf{u}_{M_{\text{cmd0}}}(t) = k(t)\left(\mathbf{v}_M(t) \times \hat{\mathbf{v}}_{MCC}(t)\right) \times \mathbf{v}_M(t) \tag{21}$$

where $k(t)$ represents the feedback gain.

Considering vertical launch, a sufficiently large lateral acceleration command should be generated i) to perform the initial turn during the boost phase following launch, and ii) to enable sufficiently fast tracking of the desired vertical flight path angle which is modified to satisfy the maximum altitude limit. However, if the gain is designed as $k(t) = \frac{N}{\|\mathbf{r}(t)\|}$ for a given constant $N$, which corresponds to the case of the pure PNG, the feedback gain attains a small value in the initial phase due to the large initial distance to the target, and as a consequence, the lateral acceleration command also becomes small. For this reason, the magnitude of the feedback gain should be greater than or equal to a certain minimum value even in the initial phase to apply the guidance command of Eq. (21) throughout the entire flight from the beginning of boost phase.

Assuming that there is no discrepancy between the actual lateral acceleration and the lateral acceleration command in Eq. (21), gravitational acceleration can be neglected, and the error between the desired and the current flight path angle is small, the time-derivative of the missile's vertical flight path angle $\gamma_M$ resulting from the given guidance law can be expressed as follows:

$$\dot{\gamma}_M(t) \approx k(t) V_M(t) \sin\left(\gamma_{MCC}(t) - \gamma_M(t)\right) \approx k(t) V_M(t) \left(\gamma_{MCC}(t) - \gamma_M(t)\right) \tag{22}$$

Given that the closed-loop response of vertical flight path angle approximately follows a linear first-order lag model, the time constant $\tau_\gamma$ and the gain $k$ are related as

$$k(t) = \frac{1}{V_M(t)\,\tau_\gamma} \tag{23}$$

In light of Eq. (23), $k \geq \frac{1}{V_M \tau_{\gamma_{\max}}}$ should be satisfied to make the effective time constant of the vertical flight path angle dynamics less than $\tau_{\gamma_{\max}}$. The allowable minimum value of $k$ can be determined from this condition.

From the aforementioned discussions, the feedback gain can be designed as

$$k\left(t\right)=\max\left(\frac{N}{\left\|\mathbf{r}\left(t\right)\right\|},\frac{1}{V_{M}\left(t\right)\tau_{\gamma_{\max}}}\right) \tag{24}$$

Lastly, a command limiter can be employed to prevent excessive lateral acceleration command that may lead the vehicle to instabilities as

$$\mathbf{u}_{M_{\text{cmd}}}\left(t\right)=\min\left(\left\|\mathbf{u}_{M_{\text{cmd0}}}\left(t\right)\right\|,u_{M_{\max}}\left(\mathsf{M}\left(t\right),Z_{M}\left(t\right)\right)\right)\frac{\mathbf{u}_{M_{\text{cmd0}}}\left(t\right)}{\left\|\mathbf{u}_{M_{\text{cmd0}}}\left(t\right)\right\|} \tag{25}$$

where $\mathbf{u}_{M_{\text{cmd0}}}$ is the original command given by Eq. (21), $\mathbf{u}_{M_{\text{cmd}}}$ denotes the magnitude-limited lateral acceleration command, and $u_{M_{\max}}$ denotes the table of maximum lateral acceleration given as a function of Mach number $\mathsf{M}\left(t\right)$ and altitude $Z_{M}\left(t\right)$.

In the following, Algorithm 2 summarises the proposed guidance method.

**Algorithm 2:** Three-Dimensional Guidance Method for Increasing Final Speed and Satisfying Altitude Limit

**Data:** $V_{\text{nominal}}$, $\rho_{sw_0}$, $\rho_{sw_f}$, $Z_{\max}$, $Z_{\text{act}}$, $n$, $N$, $\tau_{\gamma_{\max}}$, $u_{M_{\max}}$

**Input:** $\mathbf{r}_M$, $\mathbf{v}_M$, $\mathbf{r}_T$, $\mathbf{v}_T$, $\mathsf{M}$

**Output:** $\mathbf{u}_{M_{\text{cmd}}}\left(t\right)$

$\bar{V}_M \leftarrow$ Eq. (14)

$t_{go_{SCC}} \leftarrow$ Eq. (13)

$\mathbf{v}_{GCC} \leftarrow$ Eq. (16)

$\mathbf{v}_{SCC} \leftarrow$ Eq. (12)

$\mathbf{v}_{CC0} \leftarrow$ Eq. (17)

$\gamma_{CC0} \leftarrow$ Eq. (18)

$\gamma_{MCC} \leftarrow$ Algorithm 1

$\hat{\mathbf{i}}_{MCC} \leftarrow$ Eq. (20)

$\hat{\mathbf{v}}_{MCC} \leftarrow$ Eq. (19)

$k \leftarrow$ Eq. (24)

$\mathbf{u}_{M_{\text{cmd0}}}\left(t\right) \leftarrow$ Eq. (21)

$\mathbf{u}_{M_{\text{cmd}}}\left(t\right) \leftarrow$ Eq. (25)

## III. Numerical Simulation

This section presents numerical simulation results to demonstrate the performance of the proposed guidance method using a three-dimensional point-mass dynamics model.

### A. Simulation Model

A three-dimensional point-mass dynamics which includes the basic components of the lift and drag coefficients provides sufficient fidelity as a simulation model to validate the performance of a guidance algorithm. However, pseudo-measurement information for the angle-of-attack is necessary to evaluate i) the thrust that acts along the body $x$-axis rather than the velocity, and ii) the lift and drag coefficients which are given as tables of data indexed by the Mach number and the angle-of-attack in a point-mass dynamics model that does not consider rigid-body attitude and rotation. To verify the performance of a guidance law, the angle-of-attack that corresponds to the instantaneous lift acceleration should be obtained.

This study describes a physically consistent simulation model for the three-dimensional point-mass dynamics under the assumption of zero aerodynamic bank angle. The procedure to synthetically calculate the angle-of-attack is more involved in the three-dimensional point-mass dynamics model than the two-dimensional point-mass dynamics for longitudinal motion.

The proposed modelling approach is to introduce the concept of angular velocity for the three-dimensional rotation of the lift acceleration. This approach is particularly useful to approximately describe the autopilot lag in the response of the actual lift acceleration with respect to the commanded lift acceleration in three-dimensional space for a missile with skid-to-turn configuration since the lag in the lift acceleration response can be incorporated using a simple model such as the first-order linear dynamics without resolving the acceleration vector in each coordinate axis.

Algorithm 3 describes the proposed method for evaluating the equation of motion for the missile. In Algorithm 3, $\mathbf{a}_L$ and $\mathbf{a}_D$ denote the lift and drag acceleration vectors, respectively, $\boldsymbol{\omega}_L$ denotes the angular velocity of $\mathbf{a}_L$, $\mathbf{x}_M := \begin{bmatrix} \mathbf{r}_M^T & \mathbf{v}_M^T & \boldsymbol{\omega}_L^T \end{bmatrix}^T$ denotes the state vector, $V_{snd}$ denotes the speed of sound, $F_T$ denotes the thrust, $\hat{\mathbf{i}}_B$ denotes the unit vector in the direction of virtual body $x$-axis, and $\tau_{\omega_L}$ denotes the time constant for the simplified three-dimensional acceleration tracking dynamics. Also, the functions $\mathrm{atmos}$, $\mathrm{interp1}$, and $\mathrm{interp2}$ represent the altitude-dependent atmospheric model evaluation, one-dimensional and two-dimensional interpolation, respectively.

### B. Simulation Setup

Numerical simulation is performed considering a constant velocity model for the target motion. The target is considered to be cruising at a constant altitude. Two simulation cases are considered to validate the performance of the proposed guidance method for a wide range of initial conditions depending on the initial position and heading of the target. The initial $Y$-axis coordinate of the target denoted by $Y_{T_0}$ is varied in Case 1, whereas the initial horizontal heading of thed target denoted by $\chi_{T_0}$ is varied in Case 2. Also, another case is devoted to performance comparison with existing methods. In Case 3, the pure

**Algorithm 3:** Three-Dimensional Point-Mass Dynamics

**Output:** $\dot{\mathbf{x}}_M$

$[\rho(Z_M), V_{snd}(Z_M)] = \text{atmos}(Z_M)$

$Q = \frac{1}{2}\rho(Z_M)\|\mathbf{v}_M\|^2$, $\mathsf{M} = \frac{\|\mathbf{v}_M\|}{V_{snd}(Z_M)}$

$\mathbf{a}_L = \boldsymbol{\omega}_L \times \mathbf{v}_M$

$C_L = \frac{m\|\mathbf{a}_L\|}{QS_{ref}}$

$C_L^{\text{table}}\big|_{\mathsf{M}} = \text{interp2}\left(\alpha^{\text{table}}, \mathsf{M}^{\text{table}}, C_L^{\text{table}}; \alpha^{\text{table}}, \mathsf{M}\right)$

$\alpha = \text{interp1}\left(C_L^{\text{table}}\big|_{\mathsf{M}}, \alpha^{\text{table}}; C_L\right)$

$C_D = \text{interp2}\left(\alpha^{\text{table}}, \mathsf{M}^{\text{table}}, C_D^{\text{table}}; \alpha, \mathsf{M}\right)$

$\mathbf{a}_D = -\frac{C_D QS_{ref}}{m}\frac{\mathbf{v}_M}{\|\mathbf{v}_M\|}$

$\hat{\mathbf{i}}_B = \cos\alpha\frac{\mathbf{v}_M}{\|\mathbf{v}_M\|} + \sin\alpha\frac{\mathbf{a}_L}{\|\mathbf{a}_L\|}$

$\mathbf{a}_M = \mathbf{a}_L + \mathbf{a}_D + \frac{F_T}{m}\hat{\mathbf{i}}_B + \mathbf{g}$

$\mathbf{a}_{L_{\text{cmd}}} = \mathbf{u}_{M_{\text{cmd}}} - \frac{\mathbf{v}_M}{\|\mathbf{v}_M\|} \times \left\{\left(\frac{F_T}{m}\hat{\mathbf{i}}_B + \mathbf{g}\right) \times \frac{\mathbf{v}_M}{\|\mathbf{v}_M\|}\right\}$

$\boldsymbol{\omega}_{L_{\text{cmd}}} = \frac{\mathbf{v}_M \times \mathbf{a}_{L_{\text{cmd}}}}{\|\mathbf{v}_M\|^2}$

$$\dot{\mathbf{x}}_M = \begin{bmatrix} \mathbf{v}_M \\ \mathbf{a}_M \\ \frac{\boldsymbol{\omega}_{L_{\text{cmd}}} - \boldsymbol{\omega}_L}{\tau_{\omega_L}} \end{bmatrix}$$

PNG and the course modification guidance law presented in [4] are tested under the same setting used in Case 1. All other simulation parameters including the initial condition of the missile, the velocity of the target, and the tunable design parameters of the guidance algorithm are fixed. The missile is launched vertically from the ground, and the guidance algorithm is applied throughout the entire flight from the launch point. Simulation is performed using the fixed-step solver ODE5 with the integration step size of $0.001$s. Simulation is stopped if the altitude increases above the upper limit $Z_{\max}$ or decreases below $0$.

### *C. Simulation Results*

*1) Case 1. Various Initial Target Position:* Figures 2-8 show the three-dimensional trajectory, the two-dimensional trajectory on the horizontal plane, the time histories of approximate time-to-go, speed, altitude, vertical flight path angle, and lift acceleration, respectively, for all initial distances tested in Case 1. Also, Figs. 9 and 10 show the detailed plots for two-dimensional trajectory, the vertical flight path angle command and the corresponding response for Case 1. All variables except the flight path angle are normalised with respect to their characteristic values. In particular, the altitude shown in Fig.

6 is normalised by the maximum altitude $Z_{\max}$. In all cases, the interception error, i.e., the distance between the missile and the target at the final time, was below $0.3$m. The results indicate that the proposed guidance algorithm generates manoeuvre patterns in both vertical and horizontal motion as intended in the design process. Notably, Figs. 2 and 6 clearly show that the guidance algorithm satisfies the maximum altitude limit in all cases. The comparison between Figs. 10a-10e shows that the desired vertical flight path angle is modified to limit the altitude increase only in the cases of long-range flight. The vertical plane motion resulting from the proposed guidance method takes the pattern consisting of ascend-cruise-descend intervals for long-distance targets.

*2) Case 2. Various Initial Target Horizontal Heading:* Figures 11-17 show the three-dimensional trajectory, the two-dimensional trajectory on the horizontal plane, the time histories of approximate time-to-go, speed, altitude, vertical flight path angle, and lift acceleration, respectively, for all initial headings tested in Case 2. Also, Figs. 18 and 19 show the detailed plots for two-dimensional trajectory, the vertical flight path angle command and the corresponding response for Case 2. The figures show the normalised variables as in Case 1. The vertically launched missile sets its course on the horizontal path from the initial time by the desired course vector tracking action of the proposed method. The results indicate that the proposed guidance method can achieve succesful interception not only for various initial positions but also for various initial horizontal headings of the target. The interception performance measured in terms of final distance between the missile and the target was below $0.3$m as in Case 1. The trajectories did not violate the maximum altitude limit in all cases as shown in Fig. 15.

*3) Case 3. Comparison with Existing Methods:* The performance of the proposed method is compared with two existing methods, namely, the pure PNG developed for homing and the course modification guidance law developed in [4] more specifically for midcourse phase. These methods are tested under the same simulation condition and the same command limiter defined by Eq. (25). First, the acceleration command for the pure PNG is given by

$$\mathbf{u}_{M_{\text{cmd0}}}(t) = N\boldsymbol{\Omega}(t) \times \mathbf{v}_M(t) = N\frac{\{\mathbf{r}(t) \times (\mathbf{v}_T(t) - \mathbf{v}_M(t))\}}{\|\mathbf{r}(t)\|^2} \times \mathbf{v}_M(t) \tag{26}$$

where $\boldsymbol{\Omega}$ represents the angular velocity of the line-of-sight vector $\mathbf{r}(t)$, and $N$ is the navigation constant. Next, the set of command equations for the course modification guidance law is given by

$$t^*_{go_{SCC}} = \frac{\mathbf{v}_T \cdot \mathbf{r}(t) + \sqrt{(\mathbf{v}_T \cdot \mathbf{r}(t))^2 + \left(V^2_{\text{nominal}} - V_T^2\right)\|\mathbf{r}(t)\|^2}}{V^2_{\text{nominal}} - V_T^2} \tag{27}$$

$$\mathbf{v}^*_{GCC}(t) = \frac{\mathbf{r}(t) + \mathbf{v}_T t^*_{go_{SCC}} - \frac{1}{2}\mathbf{g}{t^*_{go_{SCC}}}^2}{\frac{V_{\text{nominal}}}{V_M(t)} t^*_{go_{SCC}}} \tag{28}$$

$$\gamma^*_{GCC}(t) = \tan^{-1}\left(\frac{\mathbf{v}^*_{GCC}(t)\cdot\hat{\mathbf{k}}}{\left\|\left(\hat{\mathbf{k}}\times\mathbf{v}^*_{GCC}(t)\right)\times\hat{\mathbf{k}}\right\|}\right) \tag{29}$$

$$\gamma_e(t) = \begin{cases} \gamma_{e_0}\frac{t^*_{go_{SCC}}-T_{TG}}{t+t^*_{go_{SCC}}} & \text{if } t^*_{go_{SCC}} > T_{TG} \\ 0 & \text{if } t^*_{go_{SCC}} \le T_{TG} \end{cases} \tag{30}$$

$$\hat{\mathbf{i}}^*_{MCC}(t) = \frac{\left(\hat{\mathbf{k}}\times\mathbf{v}^*_{GCC}(t)\right)\times\hat{\mathbf{k}}}{\left\|\left(\hat{\mathbf{k}}\times\mathbf{v}^*_{GCC}(t)\right)\times\hat{\mathbf{k}}\right\|} \tag{31}$$

$$\hat{\mathbf{v}}^*_{MCC}(t) = \cos\left(\gamma^*_{GCC}(t)+\gamma_e(t)\right)\hat{\mathbf{i}}^*_{MCC}(t) + \sin\left(\gamma^*_{GCC}(t)+\gamma_e(t)\right)\hat{\mathbf{k}} \tag{32}$$

$$\mathbf{u}_{M_{\text{cmd0}}}(t) = \frac{N}{V_M(t)\,t^*_{go_{SCC}}}\left(\mathbf{v}_M(t)\times\hat{\mathbf{v}}^*_{MCC}(t)\right)\times\mathbf{v}_M(t) \tag{33}$$

where $\mathbf{v}^*_{GCC}(t)$ is the collision course vector for which the vertical flight path angle is given by $\gamma^*_{GCC}(t)$, $\gamma_e(t)$ denotes the additional elevation angle defined with respect to $\mathbf{v}^*_{GCC}(t)$, and $\hat{\mathbf{v}}^*_{MCC}(t)$ represents the modified desired course direction. In Eq. (30), $\gamma_{e_0}$ is a design parameter that determines the initial direction of desired course vector, and $T_{TG}$ is the duration of terminal phase in which no modification is added to the collision course vector. The values used for $V_{\text{nominal}}$ and $N$ are identical to those used for the proposed method and the pure PNG, respectively. A fixed value is used for $T_{TG}$ in all cases, and $\gamma_{e_0}$ is set to be $\gamma_L - \gamma^*_{GCC}(t_0)$ with a launch angle $\gamma_L$ as designed in [4].

Figures 20-24 show the three-dimensional trajectory, and the time histories of speed, altitude, vertical flight path angle, and lift acceleration obtained by adopting the pure PNG with $N = 3$. The pure PNG tends to reduce the heading error with respect to the instantaneous collision course. However, if the ideal flight path generated by the pure PNG exceeds the maximum altitude limit, the missile cannot produce the required lateral acceleration for heading error regulation because of the low air density at high altitude region. This failure mode is observed in Fig. 20 for targets located at long distances from the initial position where the missile is launched vertically. Comparison with the PNG indicates that the altitude modulation manoeuvre performed by the proposed guidance method enables the interception of the target located at a long distance which cannot be reached with the pure PNG.

Figures 25-29 show the three-dimensional trajectory, and the time histories of speed, altitude, vertical flight path angle, and lift acceleration obtained for the method of [4] with $\gamma_L = 30\,\text{deg}$. In comparison to the proposed method, the course modification guidance law achieved interception only for targets flying at short distances and exceeded the maximum altitude limit for longer ranges. In comparison to the pure PNG, elevation of the course vector by the angle of $\gamma_e$ causes the missile to raise its altitude. Nevertheless, the final outcome and the reason for failure in interception is similar to those resulting from the pure PNG.

Overall, the simulation results support that the proposed guidance method has the capability to effectively intercept a nonmanoeuvring target for a wide range of initial conditions. Successful intereception is achieved even if $V_{\text{nominal}}$ is set to be a representative constant value regardless of the initial distance as shown in this study. Tuning or scheduling of the nominal speed $V_{\text{nominal}}$ in Eq. (14), which is considered here as one of the design parameters for the guidance algorithm, may bring more improved horizontal guidance performance. Comparison to the existing guidance laws for homing and midcourse flight shows that the modifications introduced into the design elements including time-to-go estimate, desired course direction, and feedback gain together provides the proposed method with more versatility in interception.

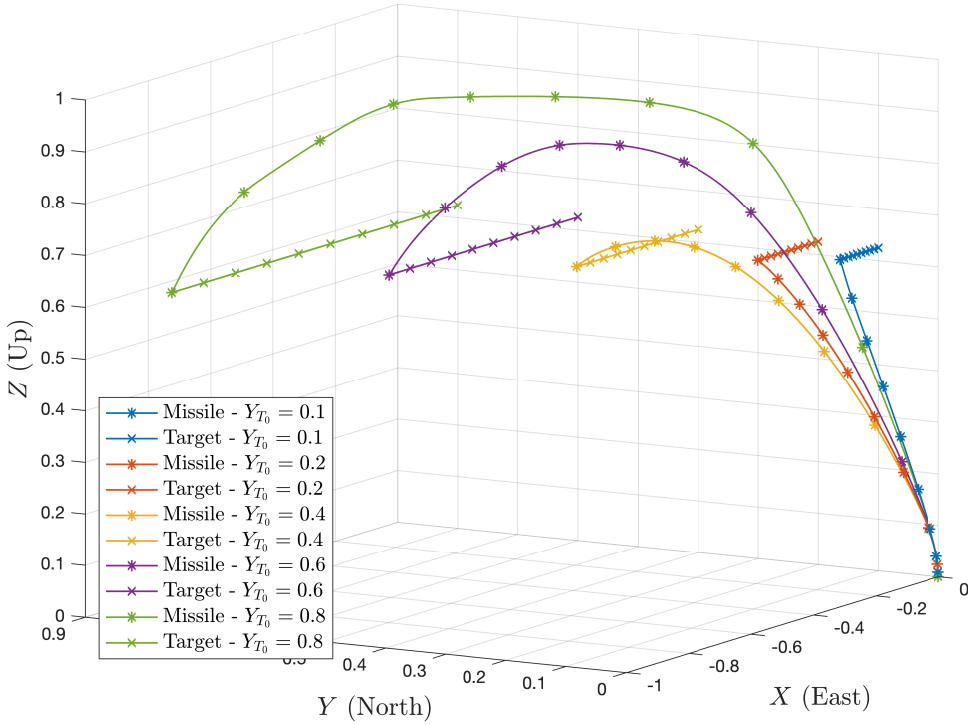


Fig. 2. Case 1. Three-Dimensional Trajectory

## IV. Conclusion

This study developed a three-dimensional guidance law for endoatmospheric target interception that is suitable for long-range anti-air missiles. More specifically, the proposed guidance law does not depend on predefined waypoints, increases altitude in the initial phase as necessary to increase the final speed, allows for satisfying the maximum altitude limit, and switches over to a terminal homing guidance law with a small heading error from the collision course. The proposed design approach can be accepted as an effective empirical method that is based on the physical understanding of the guidance response

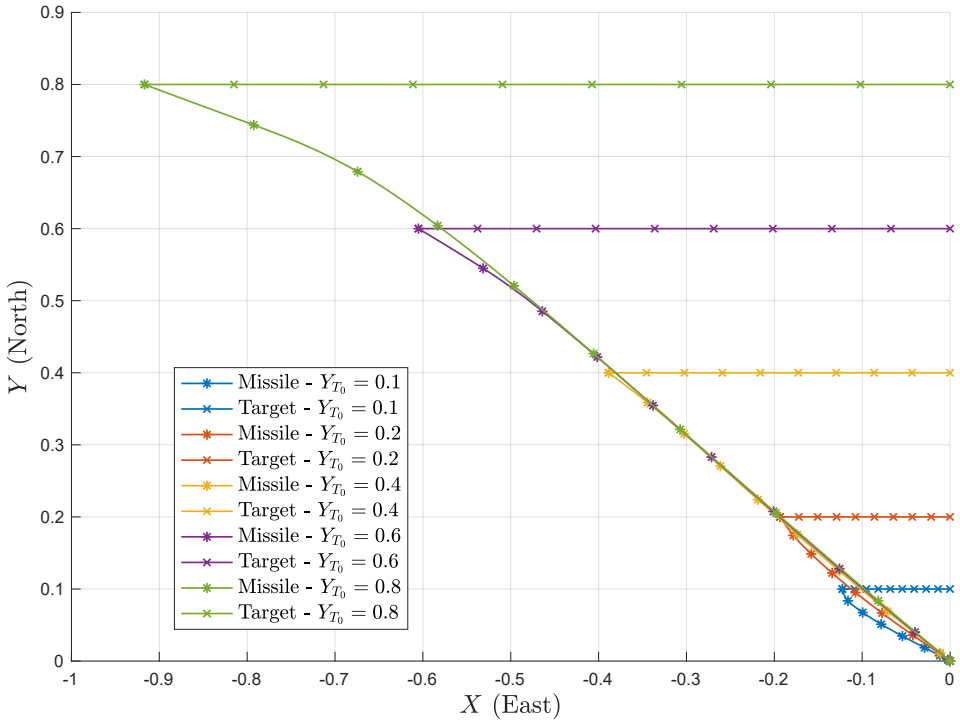


Fig. 3. Case 1. Two-Dimensional Trajectory

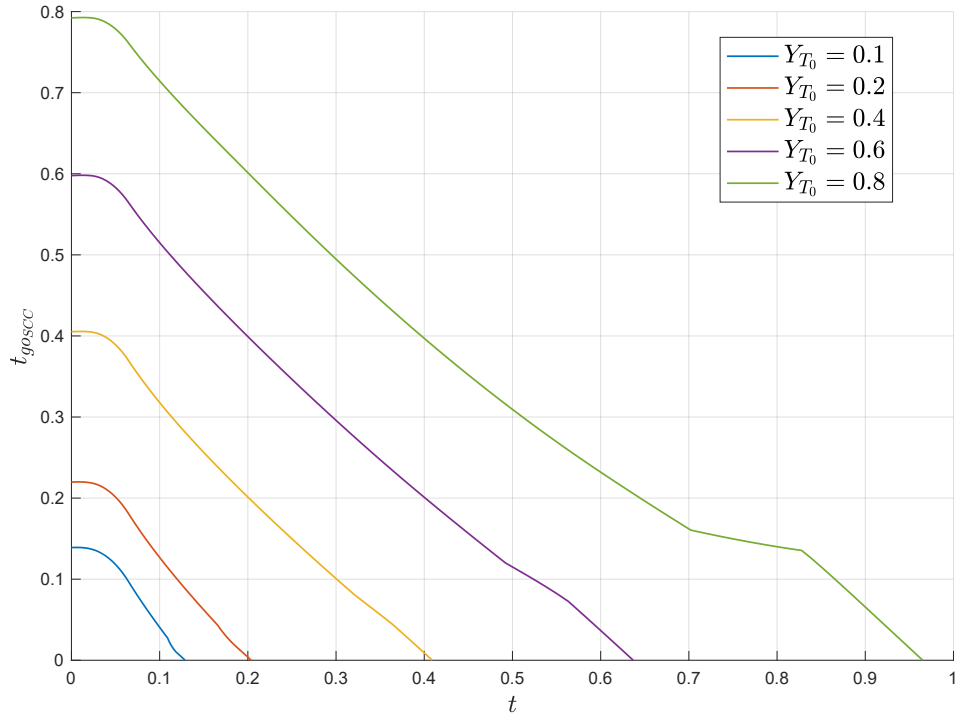


Fig. 4. Case 1. Approximate Time-to-Go History

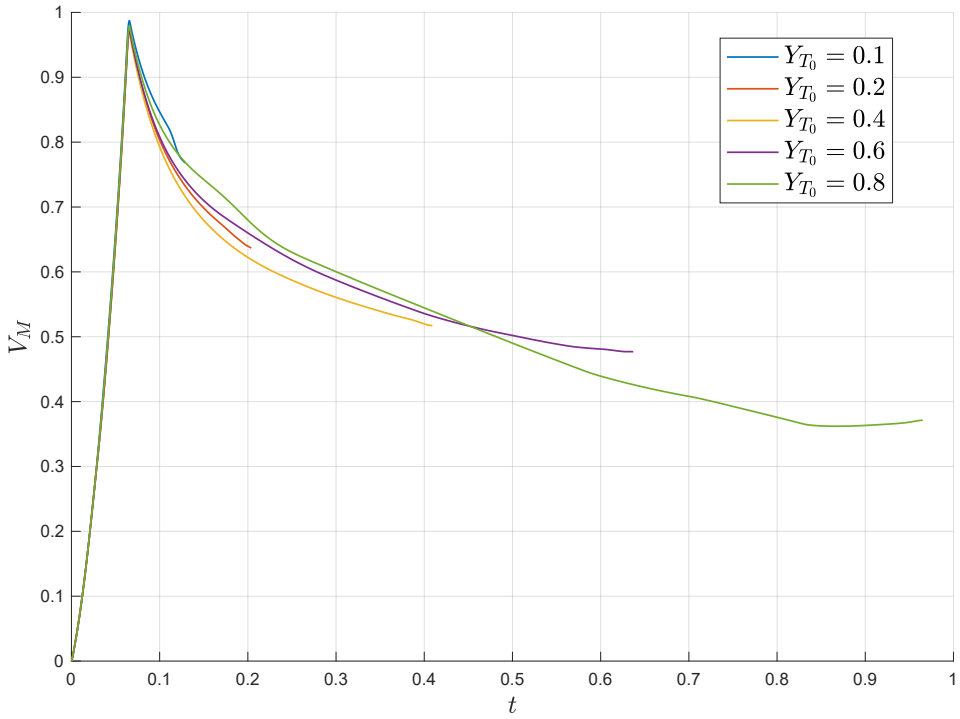


Fig. 5. Case 1. Speed History

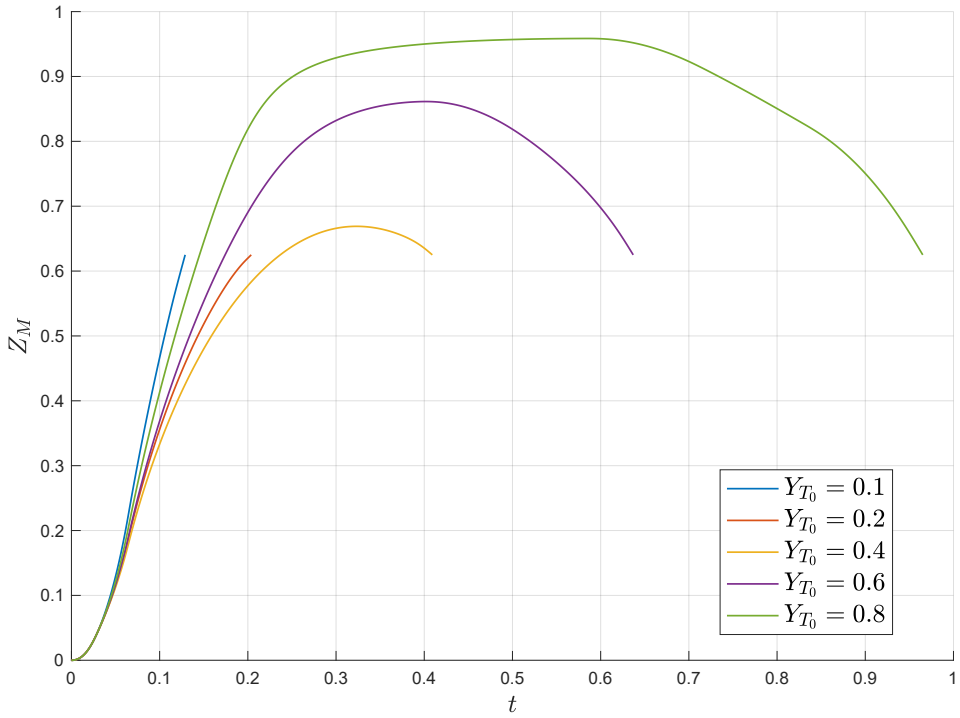


Fig. 6. Case 1. Altitude History

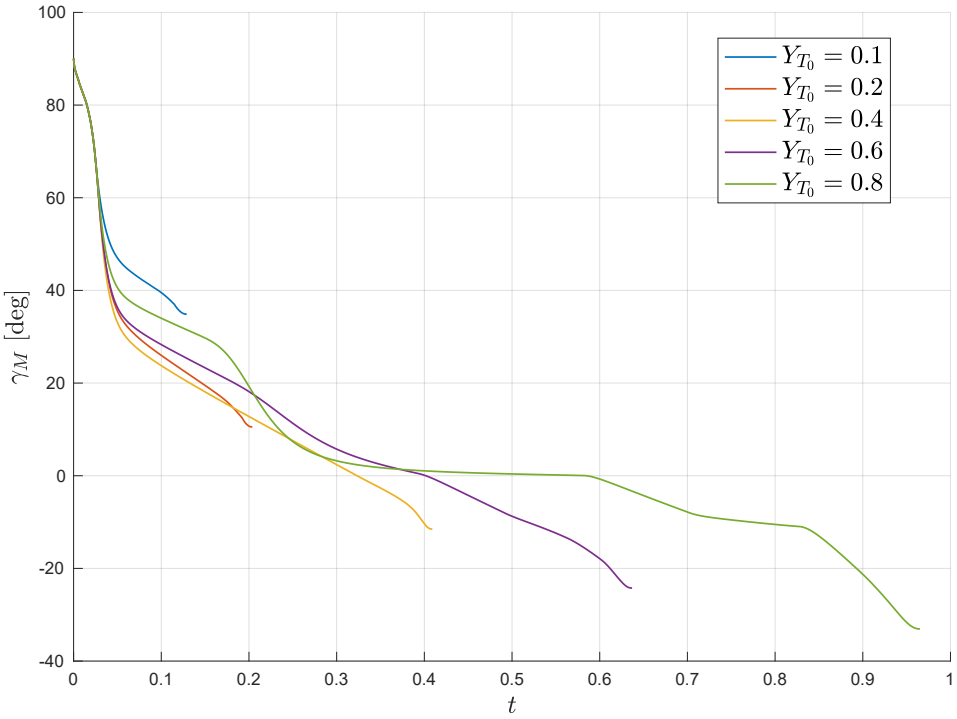


Fig. 7. Case 1. Vertical Flight Path Angle History

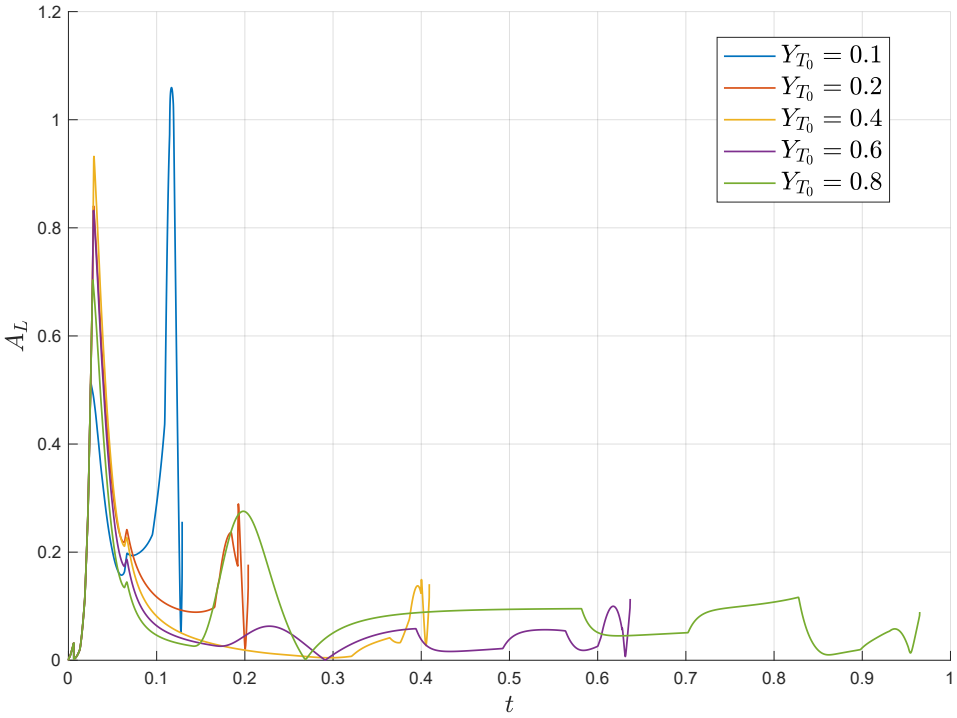


Fig. 8. Case 1. Lift Acceleration History

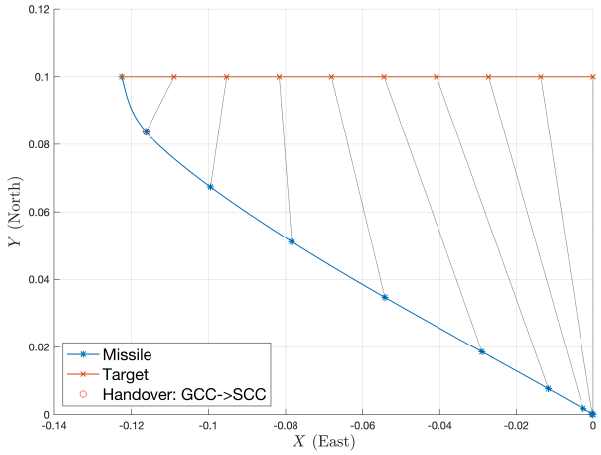


(a) $Y_{T_0} = 0.1$

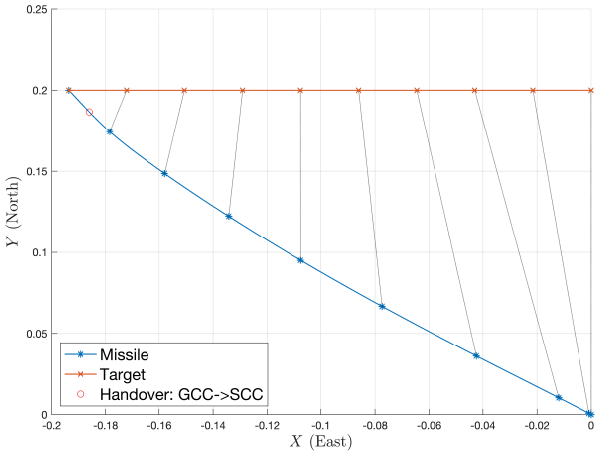


(b) $Y_{T_0} = 0.2$

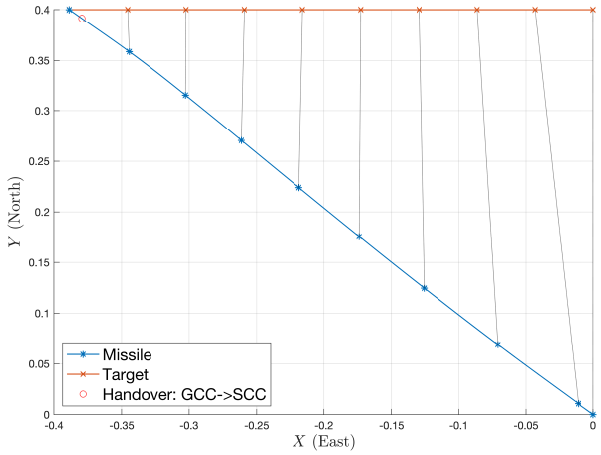


(c) $Y_{T_0} = 0.4$

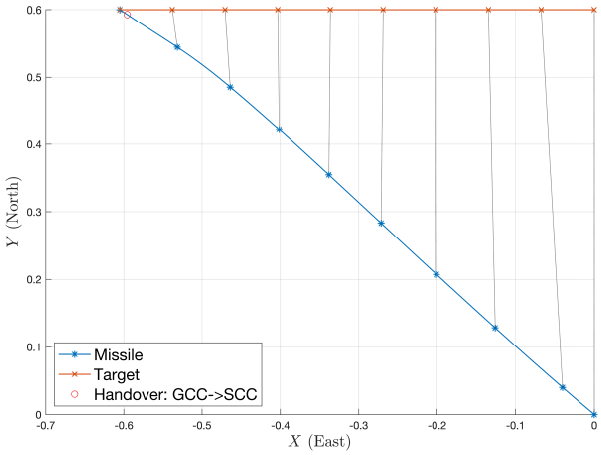


(d) $Y_{T_0} = 0.6$

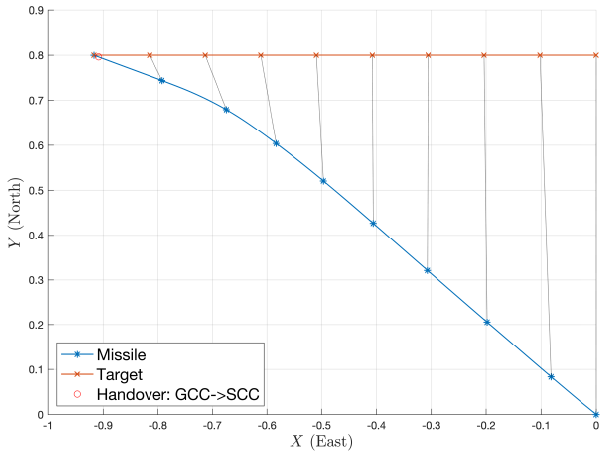


(e) $Y_{T_0} = 0.8$

Fig. 9. Case 1. Detailed Two-Dimensional Trajectory

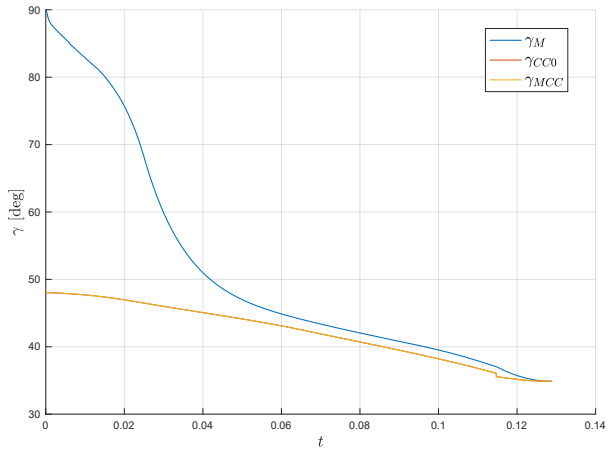


(a) $Y_{T_0} = 0.1$

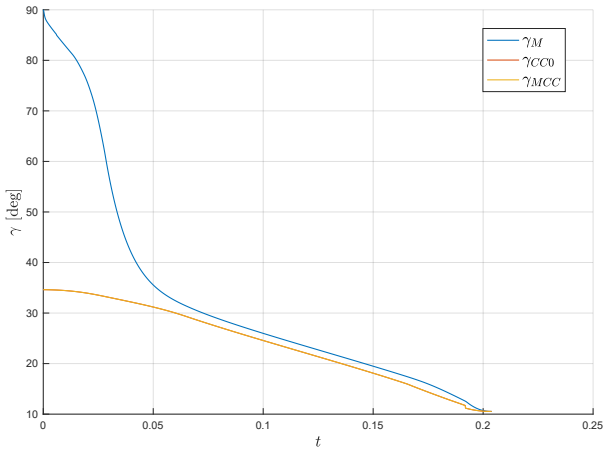


(b) $Y_{T_0} = 0.2$

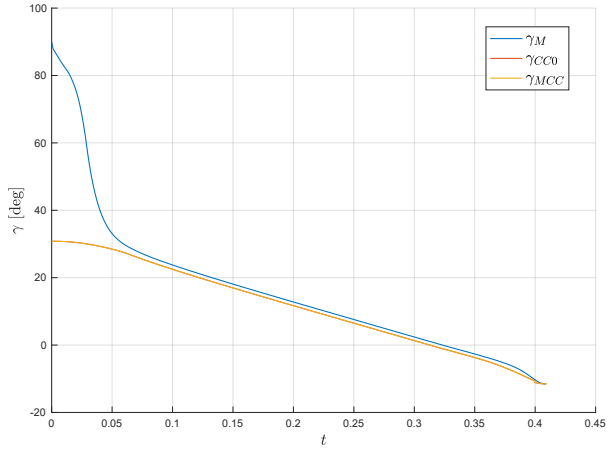


(c) $Y_{T_0} = 0.4$

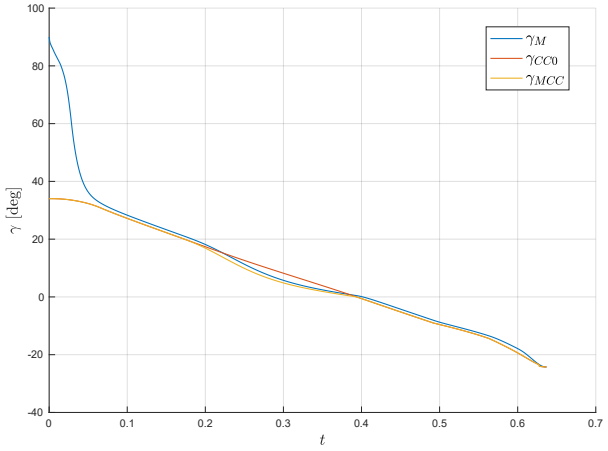


(d) $Y_{T_0} = 0.6$

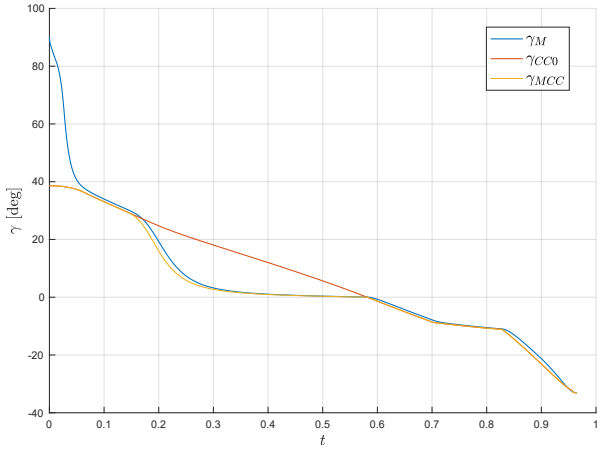


(e) $Y_{T_0} = 0.8$

Fig. 10. Case 1. Command and Response for Vertical Flight Path Angle

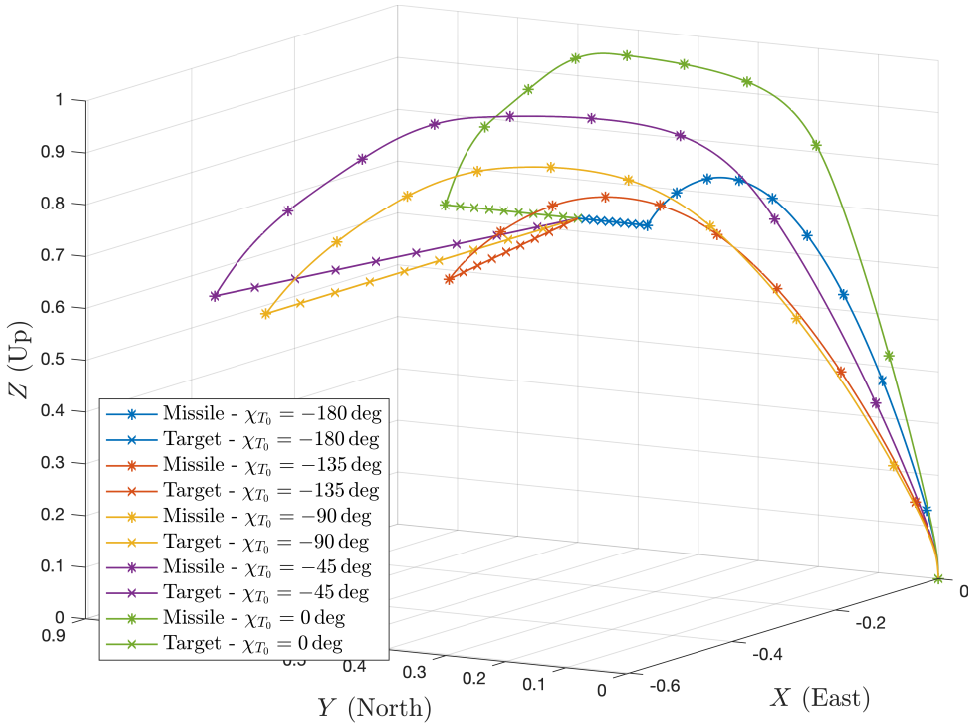


Fig. 11. Case 2. Three-Dimensional Trajectory

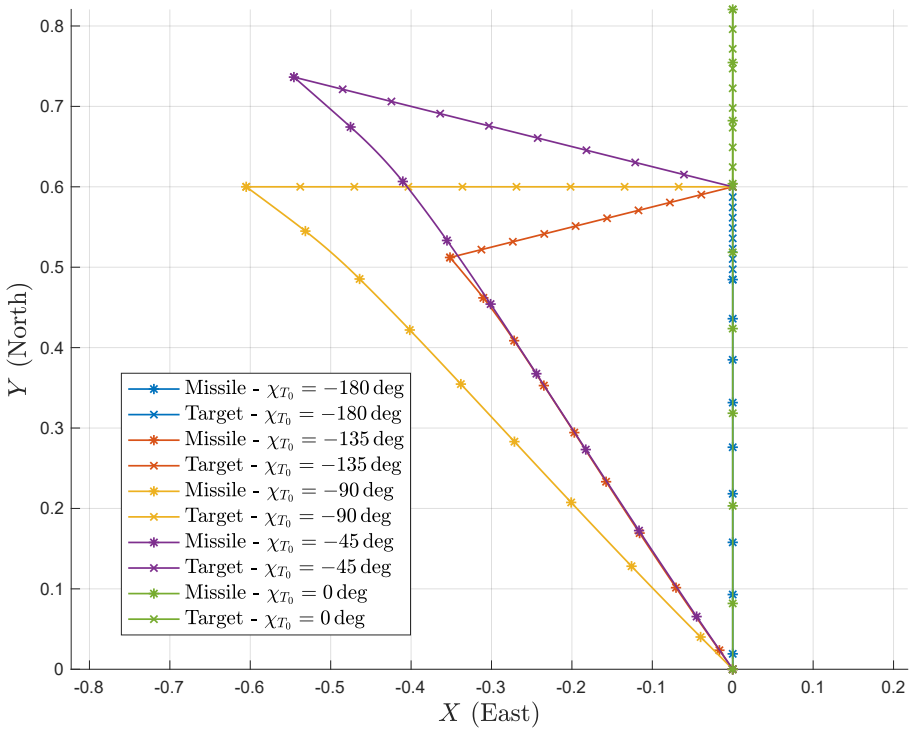


Fig. 12. Case 2. Two-Dimensional Trajectory

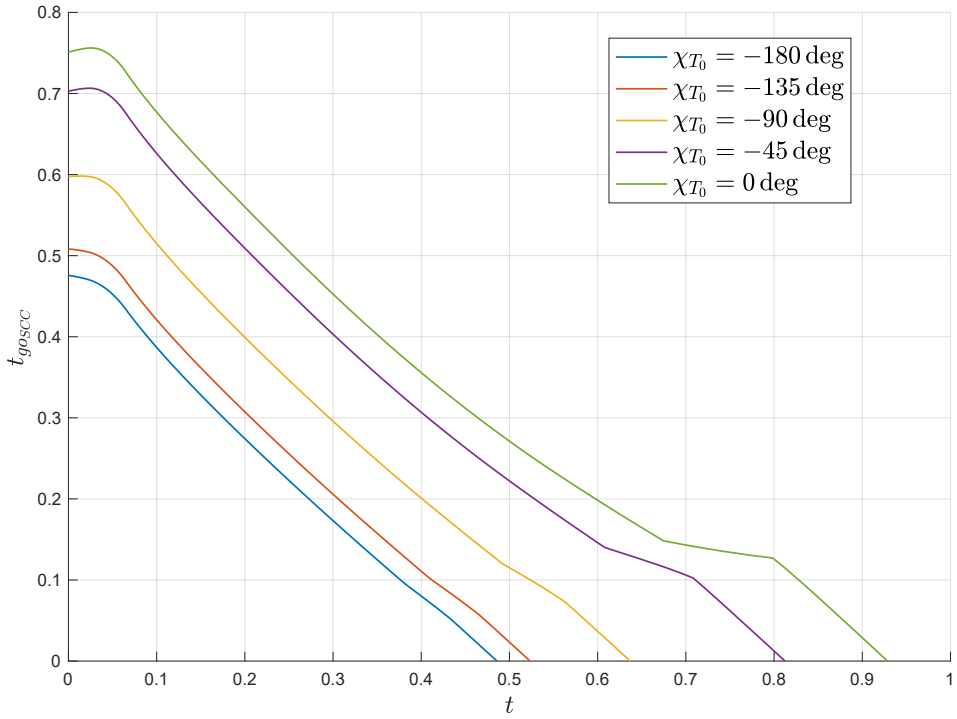


Fig. 13. Case 2. Approximate Time-to-Go History

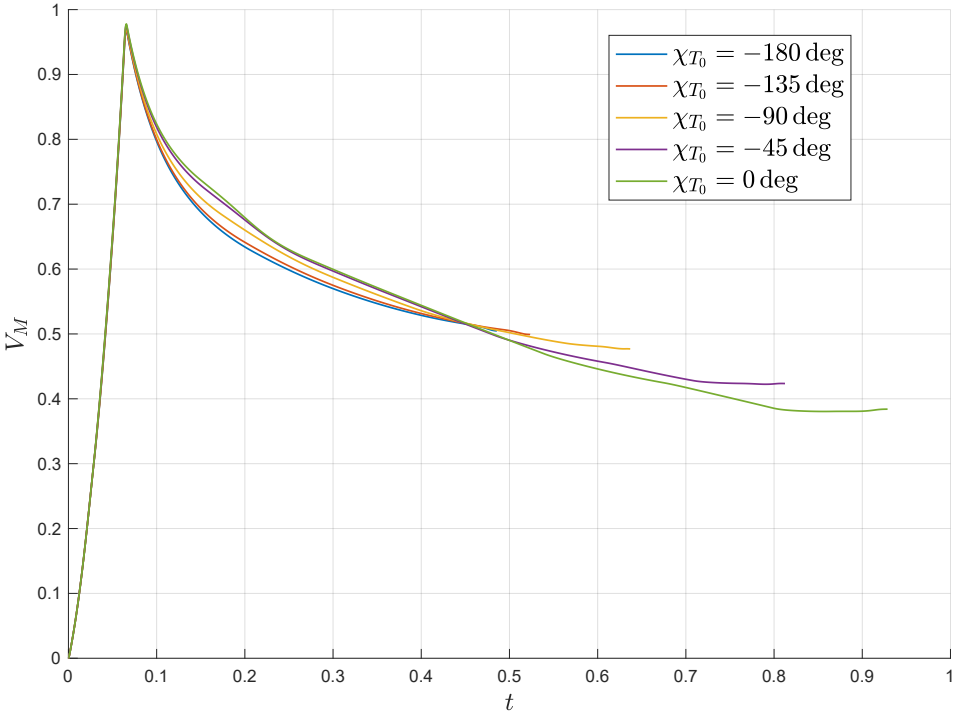


Fig. 14. Case 2. Speed History

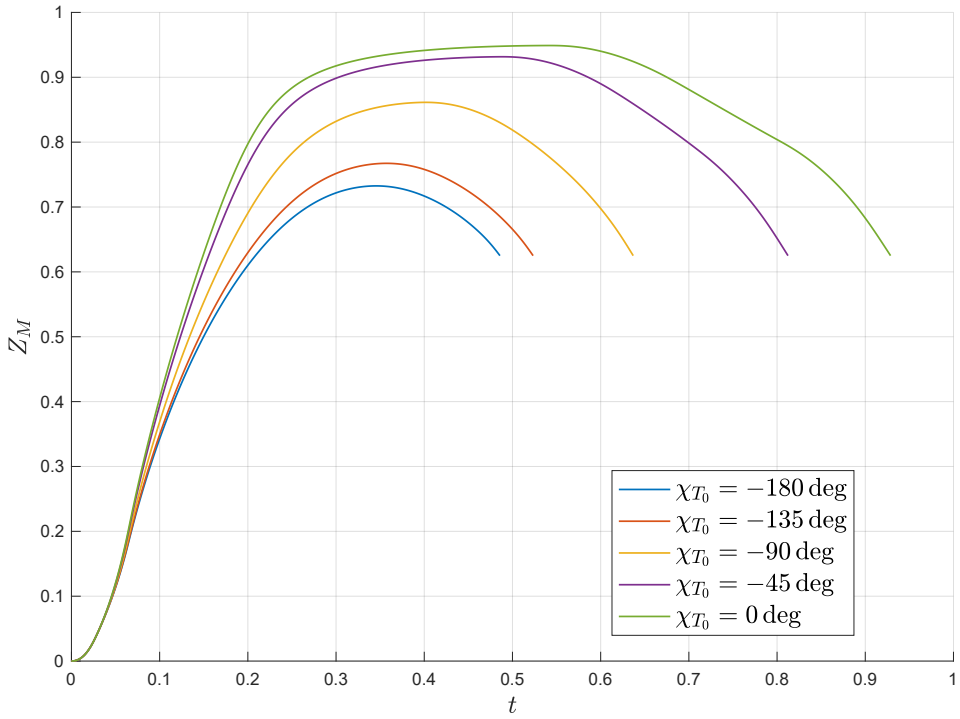


Fig. 15. Case 2. Altitude History

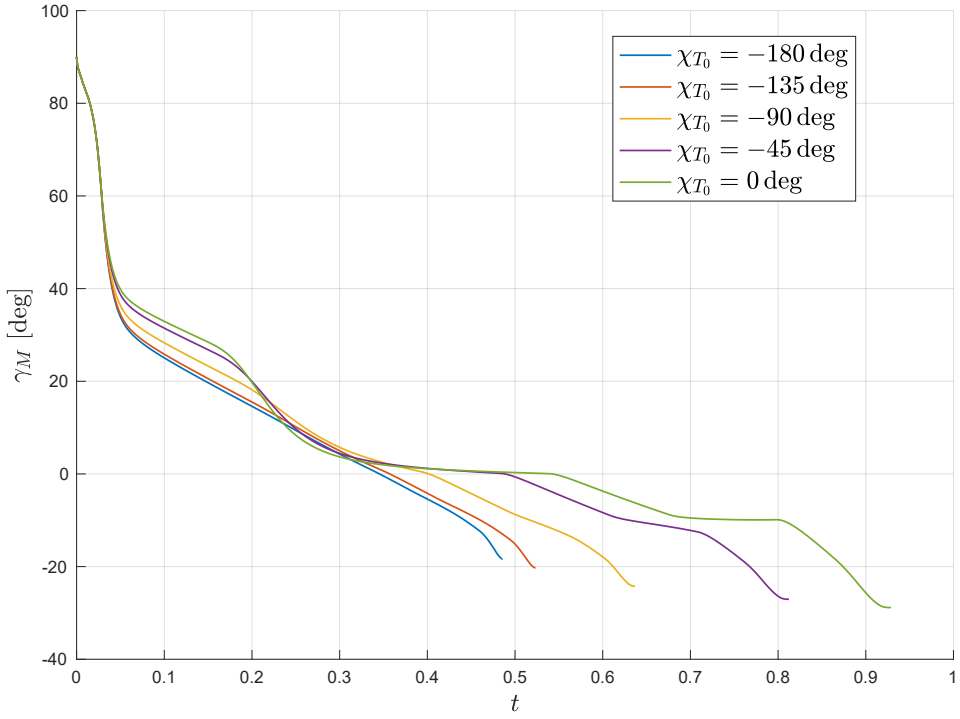


Fig. 16. Case 2. Vertical Flight Path Angle History

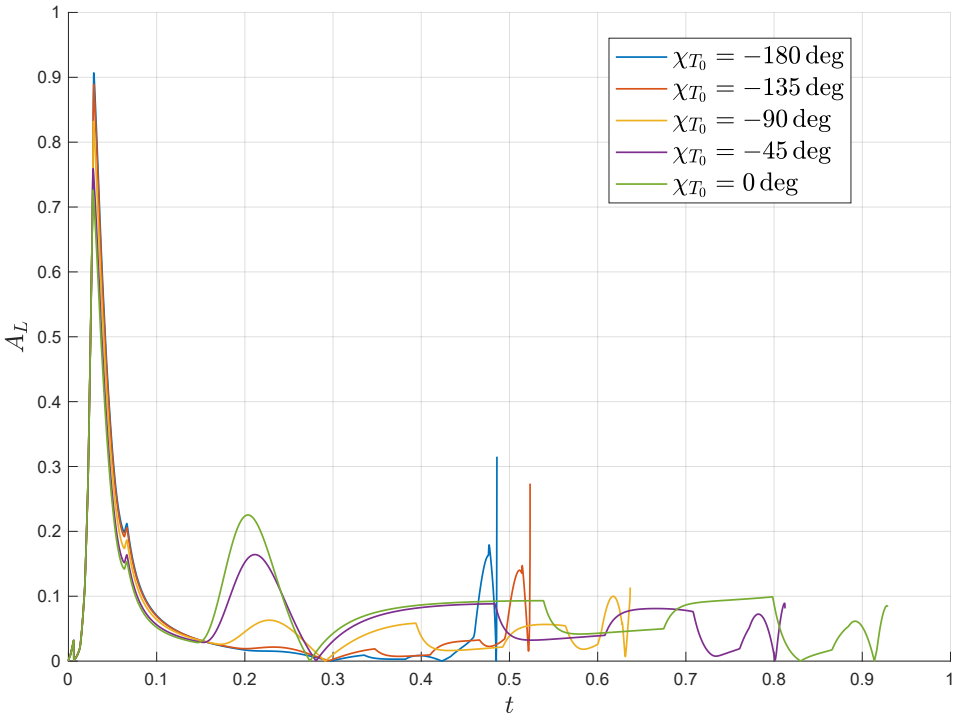


Fig. 17. Case 2. Lift Acceleration History

characteristics rather than a theoretically rigorous one. Nonetheless, the behaviour characteristics in the latter phase are similar to that expected with the PNG since the trajectory prediction based on the constant velocity model becomes more dominant as the time-to-go tends to zero. Numerical simulation illustrated that the proposed guidance method is capable of intercepting a nonmanoeuvring target for a wide range of engagement conditions. As compared to the existing methods, the proposed guidance method achieved successful interception of the target without violating the maximum altitude limit which is prescribed to avoid loss of aerodynamic control effectiveness.

## REFERENCES

[1] F. Imado, T. Kuroda, and S. Miwa, "Optimal midcourse guidance for medium-range air-to-air missiles," *Journal of Guidance, Control, and Dynamics*, vol. 13, no. 4, pp. 603–608, 1990.

[2] S. H. Jalali-Naini, "Modern midcourse guidance law with high-order dynamics," in *AIAA Guidance, Navigation, and Control Conference*, Austin, TX, USA, August 2003.

[3] S. H. Jalali-Naini and S. H. Pourtakdoust, "Modern midcourse guidance laws in the endoatmosphere," in *AIAA Guidance, Navigation, and Control Conference*, San Francisco, CA, USA, August 2005.

[4] ——, "A modified midcourse guidance law based on generalized collision course," *Journal of Aerospace Science and Technology*, vol. 3, no. 3, pp. 113–123, 2006.

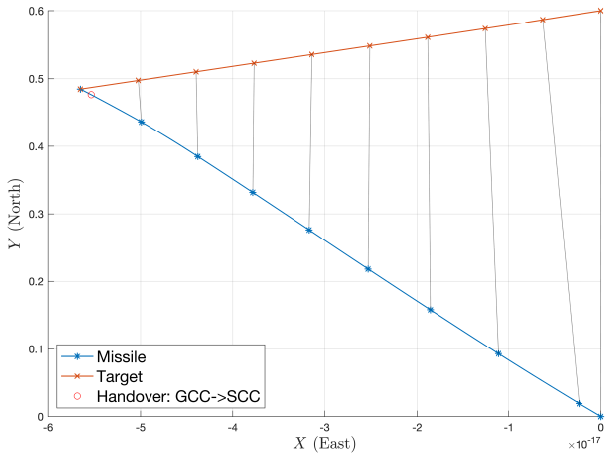


(a) $\chi_{T_0} = -180\,\text{deg}$

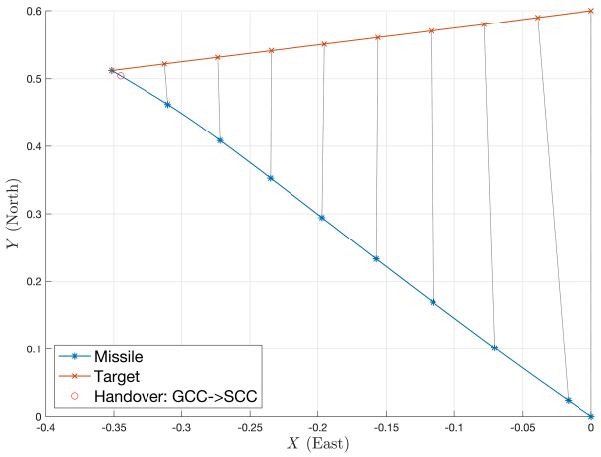


(b) $\chi_{T_0} = -135\,\text{deg}$

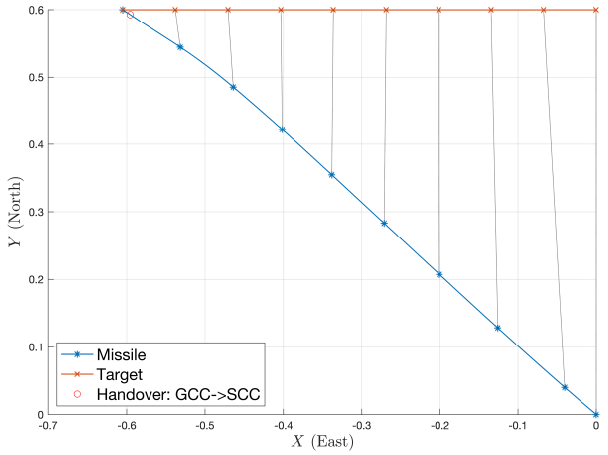


(c) $\chi_{T_0} = -90\,\text{deg}$

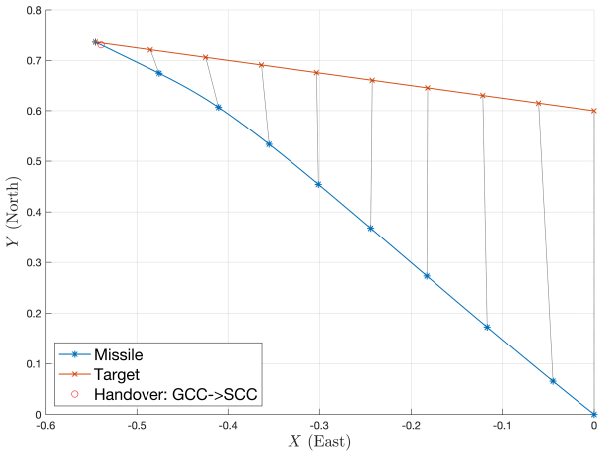


(d) $\chi_{T_0} = -45\,\text{deg}$

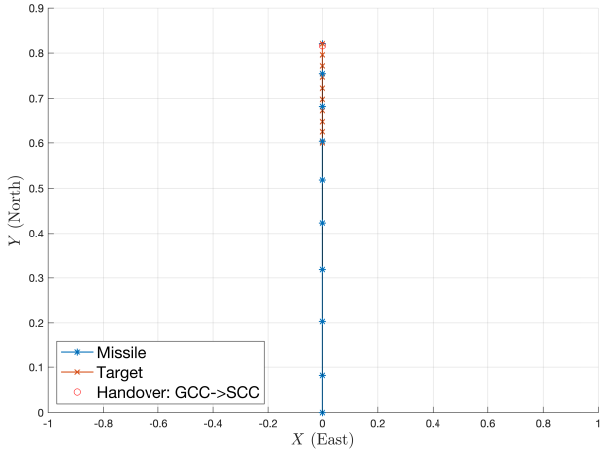


(e) $\chi_{T_0} = 0\,\text{deg}$

Fig. 18. Case 2. Detailed Two-Dimensional Trajectory

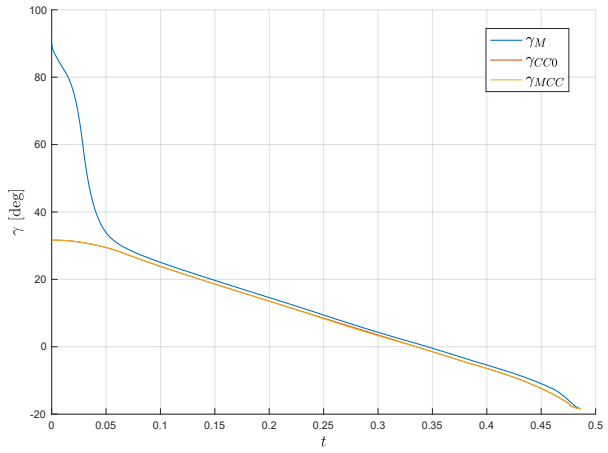


(a) $\chi_{T_0} = -180\,\text{deg}$

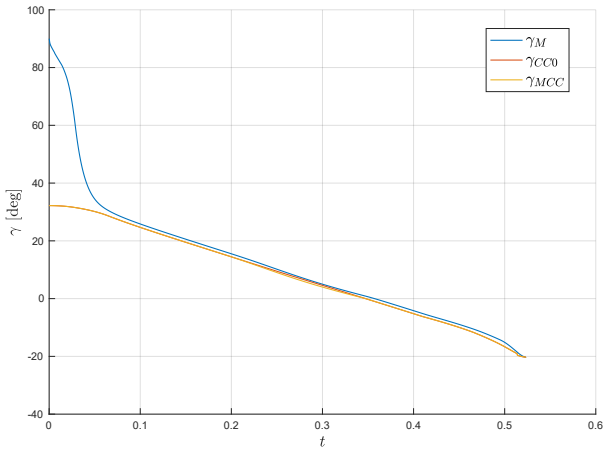


(b) $\chi_{T_0} = -135\,\text{deg}$

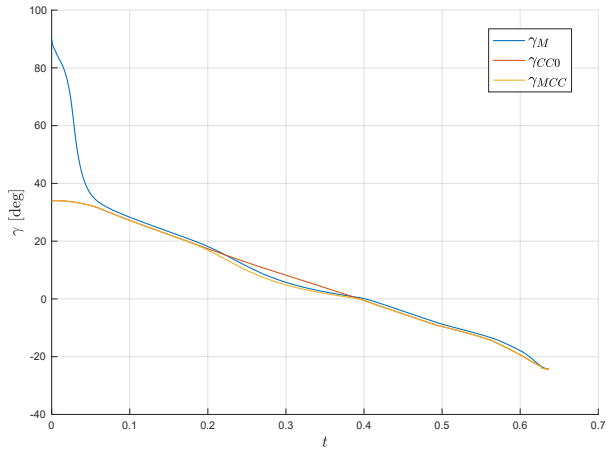


(c) $\chi_{T_0} = -90\,\text{deg}$

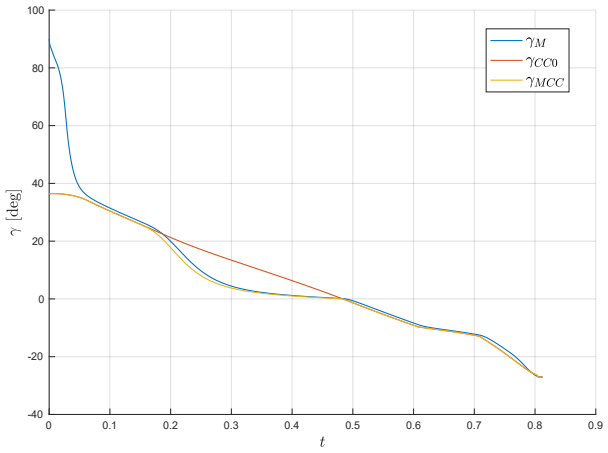


(d) $\chi_{T_0} = -45\,\text{deg}$

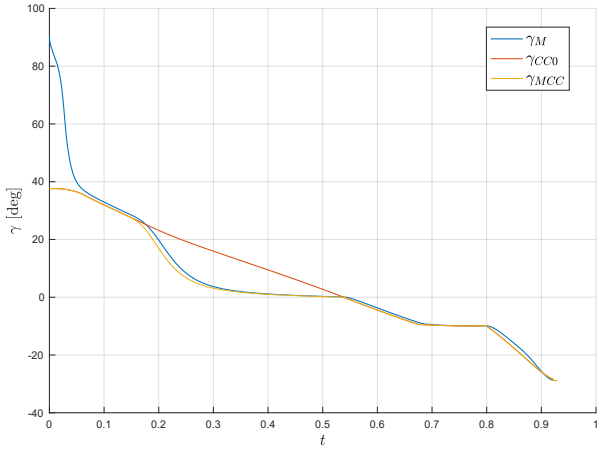


(e) $\chi_{T_0} = 0\,\text{deg}$

Fig. 19. Case 2. Command and Response for Vertical Flight Path Angle

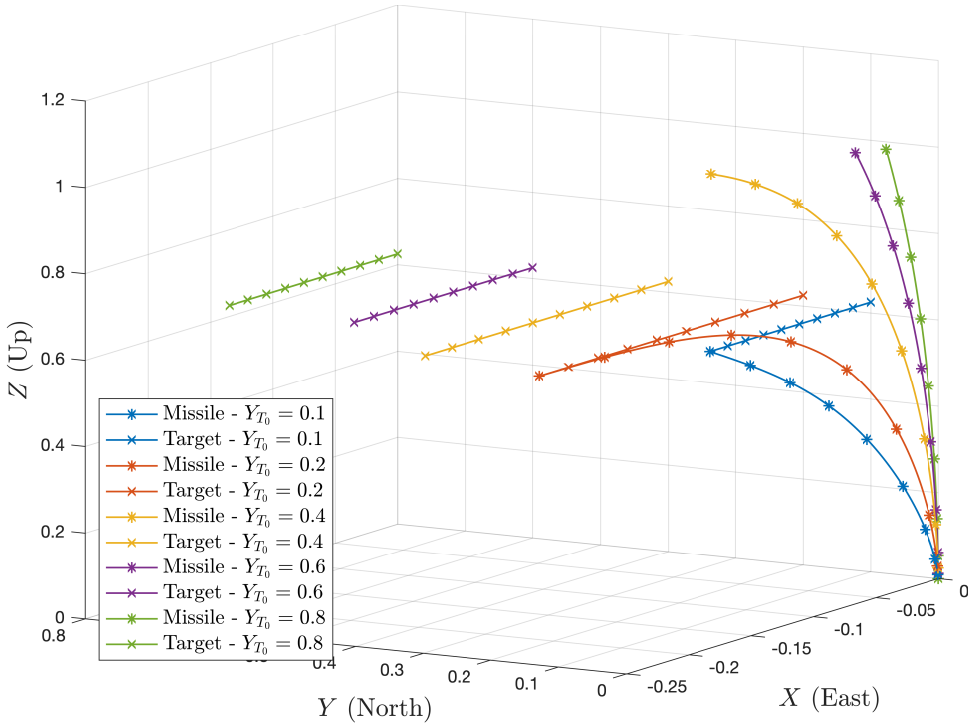


Fig. 20. Case 3. Three-Dimensional Trajectory for Pure PNG

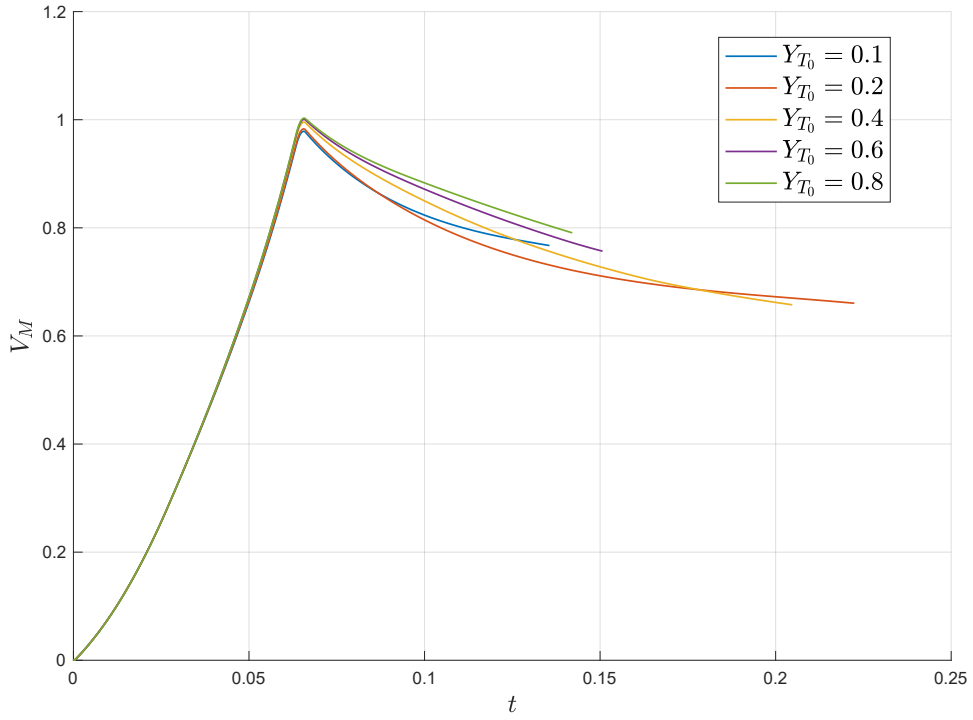


Fig. 21. Case 3. Speed History for Pure PNG

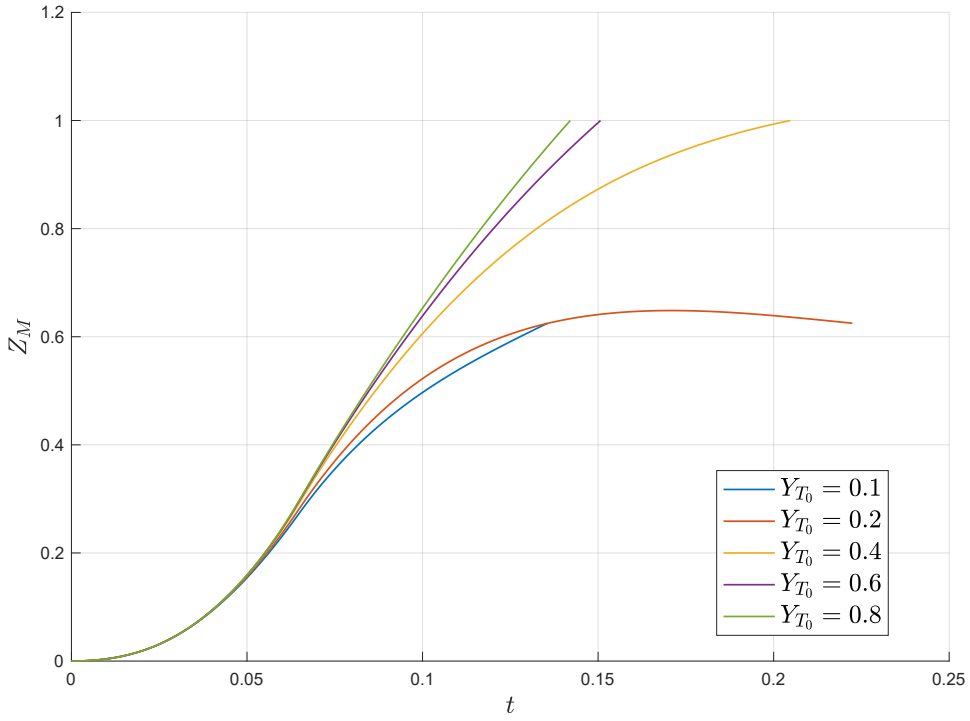


Fig. 22. Case 3. Altitude History for Pure PNG

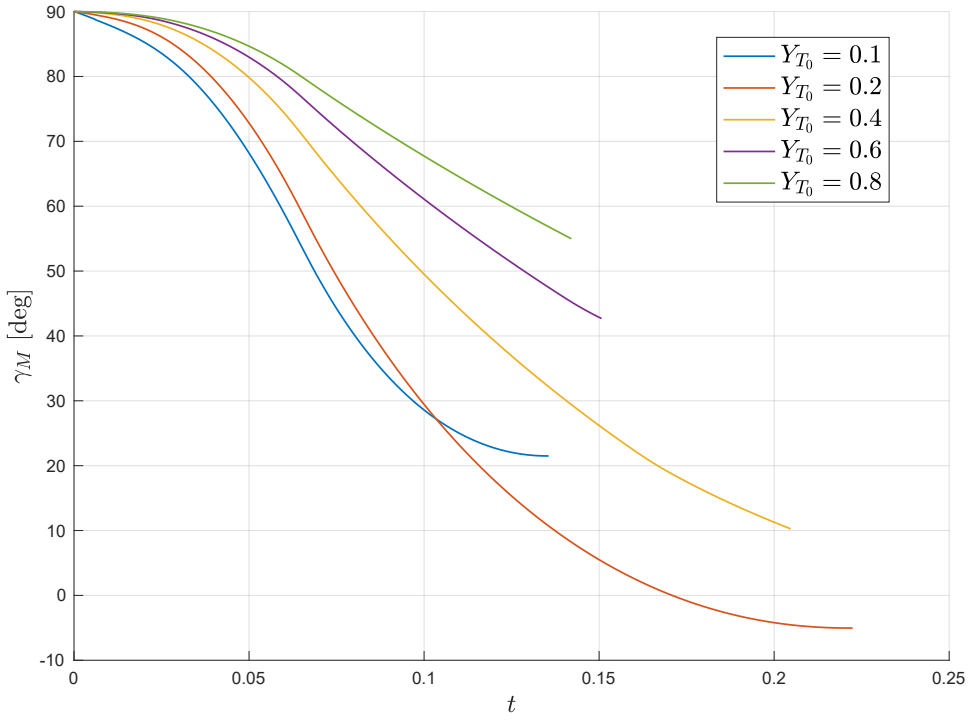


Fig. 23. Case 3. Vertical Flight Path Angle History for Pure PNG

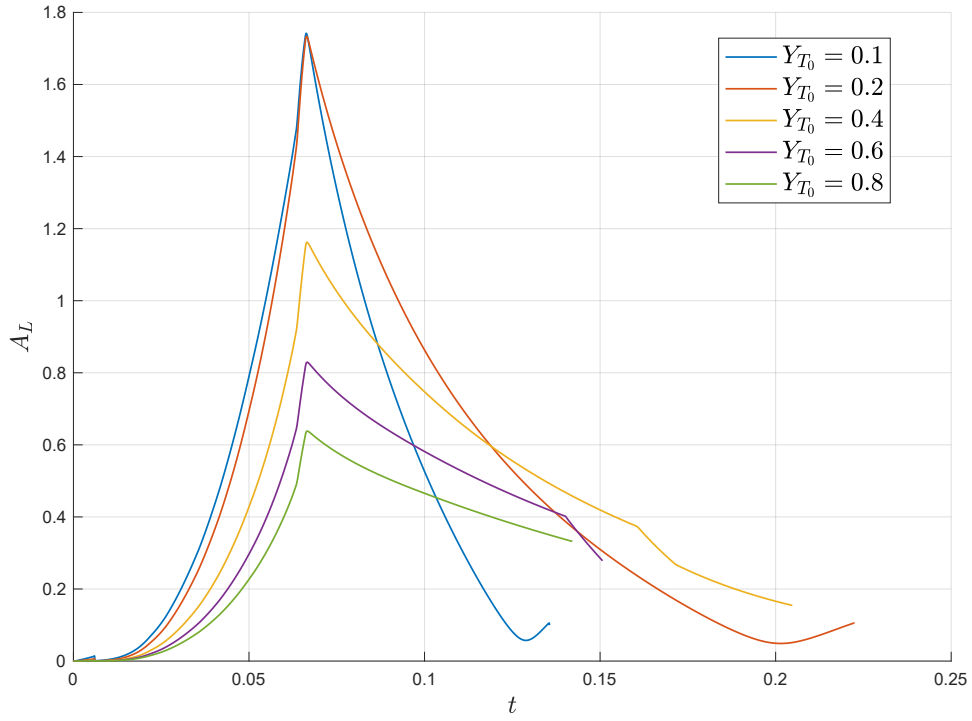


Fig. 24. Case 3. Lift Acceleration History for Pure PNG

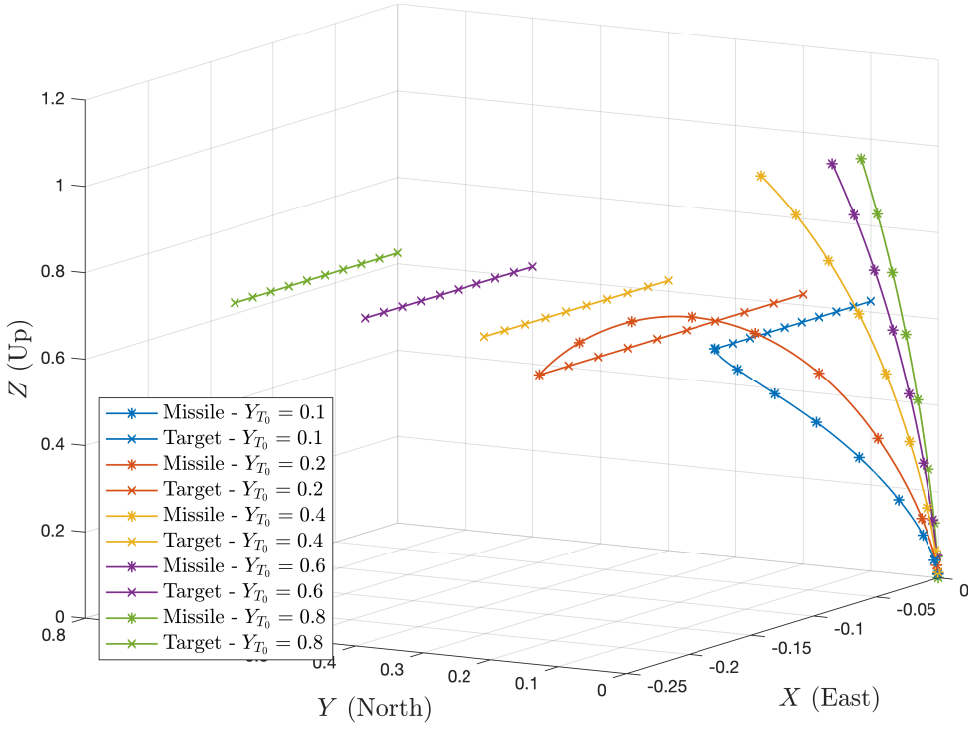


Fig. 25. Case 3. Three-Dimensional Trajectory for Course Modification Guidance Law

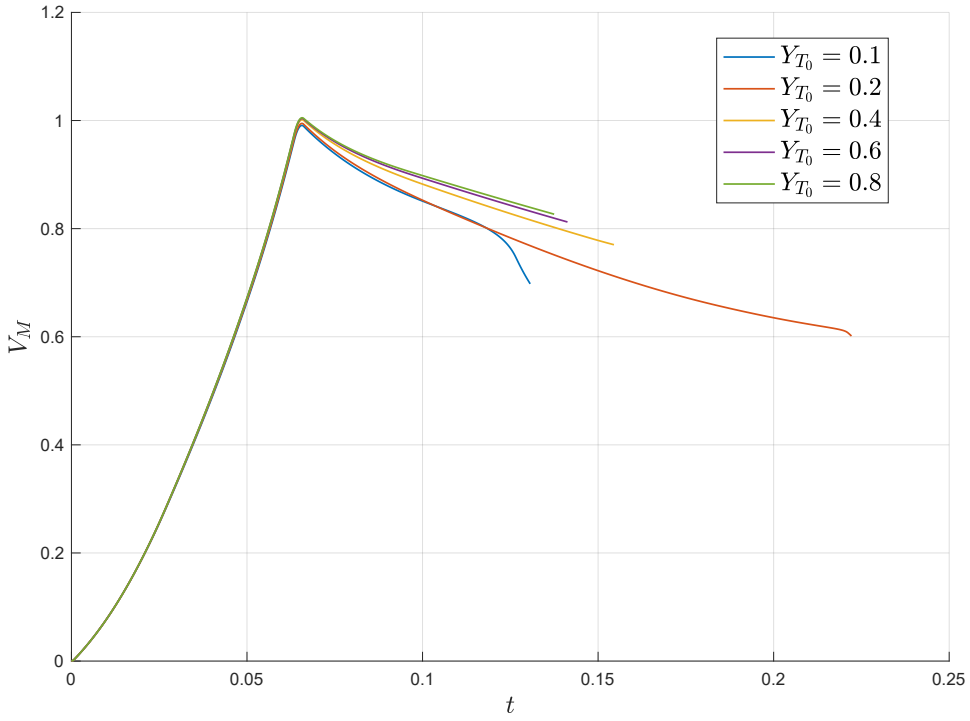


Fig. 26. Case 3. Speed History for Course Modification Guidance Law

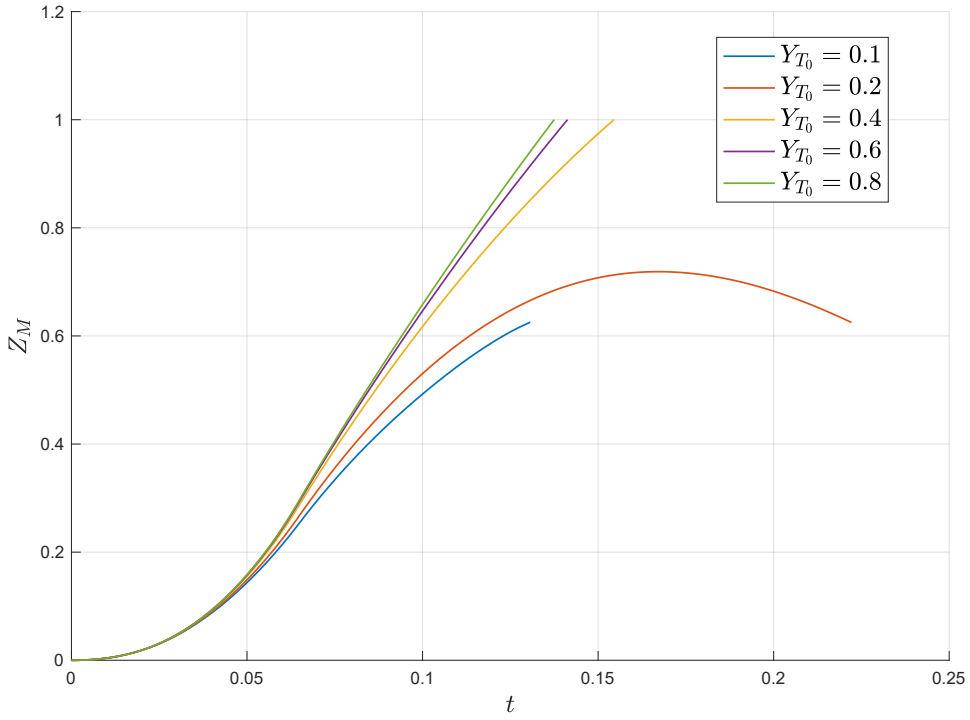


Fig. 27. Case 3. Altitude History for Course Modification Guidance Law

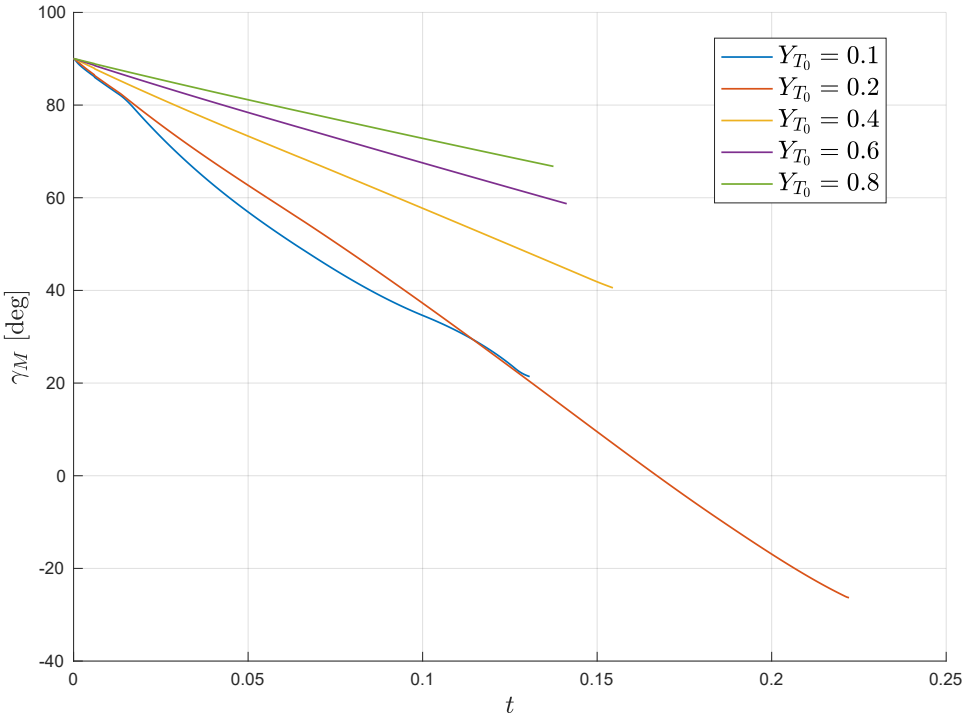


Fig. 28. Case 3. Vertical Flight Path Angle History for Course Modification Guidance Law

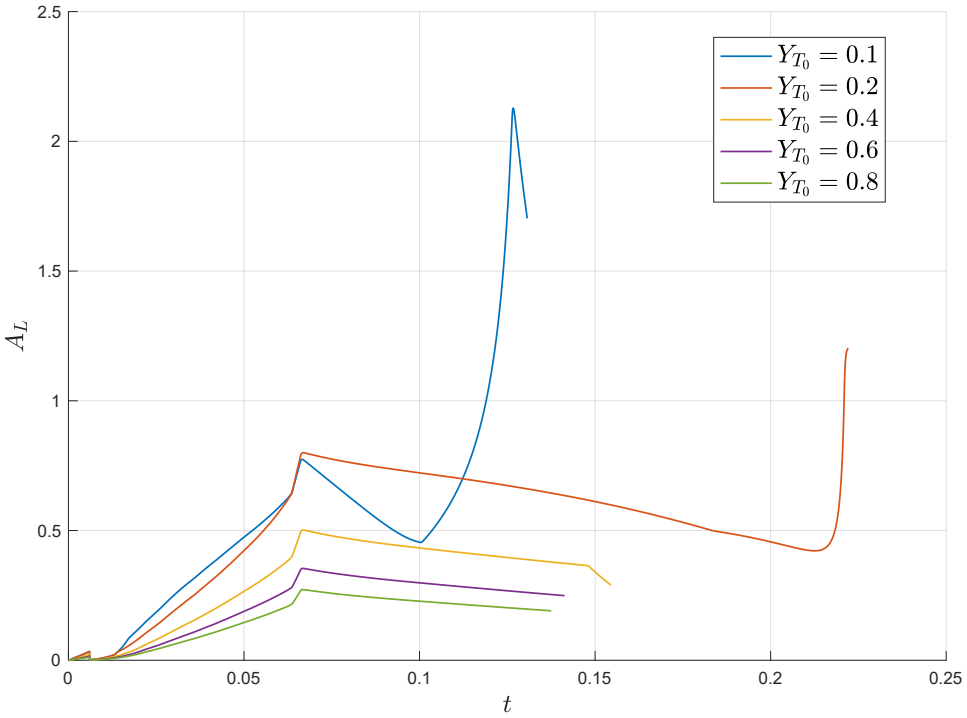


Fig. 29. Case 3. Lift Acceleration History for Course Modification Guidance Law

[5] ——, "On the predicted errors of atmospheric guidance laws," *Aircraft Engineering and Aerospace Technology*, vol. 80, no. 3, pp. 262–273, 2008.

[6] S. H. Jalali-Naini, "A trajectory shaping guidance design for midcourse phase of flight," in *The 10th Conference of Iranian Aerospace Society*, Tehran, Iran, March 2011.

[7] P. A. Raju and D. Ghose, "Empirical virtual sliding target guidance law design: An aerodynamic approach," *IEEE Transactions on Aerospace and Electronic Systems*, vol. 39, no. 4, pp. 1179–1190, 2003.

[8] N. Indig, J. Z. Ben-Asher, and N. Farber, "Near-optimal spatial midcourse guidance law with an angular constraint," *Journal of Guidance, Control, and Dynamics*, vol. 37, no. 1, pp. 214–223, 2014.

[9] V. H. L. Cheng and N. K. Gupta, "Advanced midcourse guidance for air-to-air missiles," *Journal of Guidance, Control, and Dynamics*, vol. 9, no. 2, pp. 135–142, 1986.

[10] P. K. A. Menon and M. M. Briggs, "Near-optimal midcourse guidance for air-to-air missiles," *Journal of Guidance, Control, and Dynamics*, vol. 13, no. 4, pp. 596–602, 1990.

[11] S. B. Majumder, S. M. Basha, P. K. Tiwari, D. B. N. Prasad, and A. K. Sarkar, "Practical aspects of optimal midcourse guidance for air-to-air engagement," in *4th IFAC Conference on Advances in Control and Optimization of Dynamical Systems*, Tiruchirappalli, India, February 2016.

[12] C.-F. Lin and L. L. Tsai, "Analytical solution of optimal trajectory-shaping guidance," *Journal of Guidance, Control, and Dynamics*, vol. 10, no. 1, pp. 60–66, 1987.

[13] D. Serakos and C.-F. Lin, "Linearized kappa guidance," *Journal of Guidance, Control, and Dynamics*, vol. 18, no. 5, pp. 975–980, 1995.

[14] R. W. Morgan, H. Tharp, and T. L. Vincent, "Minimum energy guidance for aerodynamically controlled missiles," *IEEE Transactions on Automatic Control*, vol. 56, no. 9, pp. 2026–2037, 2011.

[15] G. A. Harrison, "Hybrid guidance law for approach angle and time-of-arrival control," *Journal of Guidance, Control, and Dynamics*, vol. 35, no. 4, pp. 1104–1114, 2012.

[16] R. W. Morgan, "Midcourse guidance with terminal handover constraint," in *American Control Conference*, Boston, MA, USA, July 2016.

[17] ——, "Optimal position and heading control of aerospace vehicles," in *AIAA Guidance, Navigation, and Control Conference, AIAA Scitech 2020 Forum*, Orlando, FL, USA, January 2020.

[18] H.-H. Kwon and H.-L. Choi, "A convex programming approach to mid-course trajectory optimization for air-to-ground missiles," *International Journal of Aeronautical and Space Sciences*, vol. 21, pp. 479–492, 2020.

[19] H. Li, S. He, J. Wang, H.-S. Shin, and A. Tsourdos, "Near-optimal midcourse guidance for velocity maximization with constrained arrival angle," *Journal of Guidance, Control, and Dynamics*, vol. 44, no. 1, pp. 172–180, 2021.

2023-07-18

# Three-dimensional guidance method with course modification for altitude shaping in endoatmospheric interception

Cho, Namhoon

IEEE

Cho N. (2023) Three-dimensional guidance method with course modification for altitude shaping in endoatmospheric interception, IEEE Transactions on Aerospace and Electronic Systems, Available online 18 July 2023

https://doi.org/10.1109/TAES.2023.3296566